



ABCB1-dependent collateral sensitivity of multidrug-resistant colorectal cancer cells to the survivin inhibitor MX106-4C

Zi-Ning Lei^{a,b}, Najah Albadari^{c,1}, Qiu-Xu Teng^a, Hadiar Rahman^d, Jing-Quan Wang^a, Zhongzhi Wu^c, Dejian Ma^c, Suresh V. Ambudkar^d, John N.D. Wurpel^{a,*}, Yihang Pan^{b,*}, Wei Li^{c,*}, Zhe-Sheng Chen^{a,**}

^a Department of Pharmaceutical Sciences, College of Pharmacy and Health Sciences, St. John's University, Queens, NY 11439, USA

^b Guangdong Provincial Key Laboratory of Digestive Cancer Research, Digestive Diseases Center, Scientific Research Center, The Seventh Affiliated Hospital of Sun Yat-Sen University, Shenzhen, Guangdong 518107, PR China

^c Department of Pharmaceutical Sciences, University of Tennessee Health Science Center, Memphis, TN 38163, USA

^d Laboratory of Cell Biology, Center for Cancer Research, National Cancer Institute, National Institutes of Health, Bethesda, Maryland, MD 20892, USA

ARTICLE INFO

Keywords:

Colorectal cancer
ABCB1
Multidrug resistance
Collateral sensitivity
Survivin

ABSTRACT

Aims: To investigate the collateral sensitivity (CS) of ABCB1-positive multidrug resistant (MDR) colorectal cancer cells to the survivin inhibitor MX106-4C and the mechanism.

Methods: Biochemical assays (MTT, ATPase, drug accumulation/efflux, Western blot, RT-qPCR, immunofluorescence, flow cytometry) and bioinformatic analyses (mRNA-sequencing, reversed-phase protein array) were performed to investigate the hypersensitivity of ABCB1 overexpressing colorectal cancer cells to MX106-4C and the mechanisms. Synergism assay, long-term selection, and 3D tumor spheroid test were used to evaluate the anti-cancer efficacy of MX106-4C.

Results: MX106-4C selectively killed ABCB1-positive colorectal cancer cells, which could be reversed by an ABCB1 inhibitor, knockout of ABCB1, or loss-of-function ABCB1 mutation, indicating an ABCB1 expression and function-dependent mechanism. MX106-4C's selective toxicity was associated with cell cycle arrest and apoptosis through ABCB1-dependent survivin inhibition and activation on caspases-3/7 as well as modulation on p21-CDK4/6-pRb pathway. MX106-4C had good selectivity against ABCB1-positive colorectal cancer cells and retained this in multicellular tumor spheroids. In addition, MX106-4C could exert a synergistic anti-cancer effect with doxorubicin or re-sensitize ABCB1-positive cancer cells to doxorubicin by reducing ABCB1 expression in the cell population via long-term exposure.

Conclusions: MX106-4C selectively kills ABCB1-positive MDR colorectal cancer cells via a novel ABCB1-dependent survivin inhibition mechanism, providing a clue for designing CS compound as an alternative strategy to overcome ABCB1-mediated colorectal cancer MDR.

Abbreviations: 5-FU, 5-fluorouracil; ABC, ATP-binding cassette; ABCB1, ATP-binding cassette subfamily B member 1; ATP, adenosine triphosphate; BIRC5, baculoviral IAP repeat containing 5/survivin; BSA, bovine serum albumin; Bpy, 2,2'-bipyridine; CDK, cyclin dependent kinase; CDKN1A, cyclin dependent kinase inhibitor 1A (p21cip1); CI, combination index; CM-H2DCFDA, 5-(and-6)-chloromethyl-2',7'-dichlorodihydrofluorescein diacetate; CS, collateral sensitivity; DAPI, 4,6-diamidino-2-phenylindole; DEGs, differentially expressed genes; FPKM, fragments per kilobase of transcript per million mapped reads; GADD45A, growth arrest and DNA damage inducible alpha; GADD45B, growth arrest and DNA damage inducible beta; GADD45G, growth arrest and DNA damage inducible gamma; GAPDH, glyceraldehyde 3-phosphate dehydrogenase; GSH, glutathione; KEGG, Kyoto Encyclopedia of Genes and Genomes; LC-MS/MS, liquid chromatography with tandem mass spectrometry; MCTSs, multicellular tumor spheroids; MDR, multidrug resistance; MTT, 3-(4,5-Dimethylthiazol-2-yl)-2,5-diphenyltetrazolium bromide; NAC, N-acetylcysteine; PBS, phosphate buffer saline; pRb, retinoblastoma protein; ROS, reactive oxygen species; RPPA, reverse phase protein array; SI, selectivity index; TP53, tumor protein p53.

* Corresponding authors.

** Correspondence to: Department of Pharmaceutical Sciences, University of Tennessee Health Science Center, 881 Madison Avenue, room 561, Memphis, TN 38163, USA.

E-mail addresses: wurpelj@stjohns.edu (J.N.D. Wurpel), panyih@mail.sysu.edu.cn (Y. Pan), wli@uthsc.edu (W. Li), chenz@stjohns.edu (Z.-S. Chen).

¹ Present address: Department of Pharmaceutical Chemistry, College of Pharmacy, University of Hail, Hail 55473, Saudi Arabia.

<https://doi.org/10.1016/j.drug.2024.101065>

Received 1 June 2023; Received in revised form 28 January 2024; Accepted 2 February 2024

Available online 6 February 2024

1368-7646/© 2024 Elsevier Ltd. All rights reserved.

1. Introduction

Colorectal cancer is the third most commonly occurring cancer worldwide, with an estimated 1.9 million new cases and 930,000 deaths occurring in 2020 globally, accounting for 9.4% of all cancer-related deaths (Morgan et al., 2023). One of the major reasons for poor prognosis and therapy failure in colorectal cancer patients is multidrug resistance (MDR), a phenomenon in which cancer cells develop cross-resistance to anticancer drugs of different structures and pharmacological mechanisms of action (Karthika et al., 2022). Major identified mechanisms of colorectal cancer MDR include drug inactivation, drug target alternation or mutation, aberrated oncogenic or bypass signaling pathways, dysfunctional cell death pathways, and transporters-mediated reduced drug uptake or increased drug efflux (Albadari et al., 2024; Wang et al., 2022). The ATP-binding cassette (ABC) transporters are predominantly involved in drug efflux, which has become a major cause of cancer MDR (Amawi et al., 2019; Bharathiraja et al., 2023). Among the MDR-associated ABC transporters, ABCB1 (P-glycoprotein, P-gp, MDR1) is one of the most common contributors of MDR in colorectal cancer. Tumors that originated from colorectal epithelium gain intrinsic resistance to many widely used chemotherapeutic drugs that are ABCB1 substrates, such as doxorubicin, paclitaxel, and vincristine (To et al., 2020). Moreover, ABCB1 expression is inducible by exposure to chemotherapeutic agents in cancer cells resulting in acquired resistance (Efferth et al., 2020).

A variety of strategies to overcome ABCB1-mediated MDR have been investigated, including the development of drugs with a novel mechanism of action to bypass resistance and the development of novel ABCB1 inhibitors that block efflux and restore drug accumulation when given with anti-cancer drugs (Albadari et al., 2024; Zhang et al., 2021). In particular, the reversal of MDR by ABCB1 modulators has been extensively investigated. Despite showing promising results in laboratory studies, the successful translation of MDR transporter inhibition into clinical applications has been challenging because of undesirable pharmacokinetic profiles or adverse effects (Musyuni et al., 2022; Wang et al., 2019). Therefore, alternative approaches are urgently needed to circumvent or resolve cancer MDR mediated by ABCB1. In the past two decades, the discovery of small molecules that have selective toxicity against ABCB1-expressing cells but not the non-resistant parental cells, a characteristic known as collateral sensitivity (CS), has introduced an alternative strategy to surmount MDR in ABCB1 positive cancer (Efferth et al., 2020; Pluchino et al., 2012; Szakacs et al., 2014). The identification of CS compounds with high selectivity and potency may help prevent MDR when used with chemotherapeutic drugs, or re-sensitize MDR tumors to conventional treatment regimens by selectively killing MDR cells in a heterogeneous tumor population (Pluchino et al., 2012).

The discovery of more CS agents has enhanced our understanding of the mechanism for CS effects against ABCB1-positive cancer, fostering the development of this innovative approach to combat ABCB1-mediated MDR. However, there may be a tremendous difference among the mechanisms of actions by which CS compounds affect ABCB1-dependent biological events. The chemical structure has been thought to be a vital factor in categorizing CS agents of shared action mode (Furedi et al., 2017). The investigation of MDR-selective toxicity through a pharmacogenetic approach has led to the identification of the 8-hydroxyquinoline (8-OHQ) scaffold, notably associated with MDR-selective activity (Szakacs et al., 2004). Several 8-OHQ derivatives, such as NSC693871, NSC693872, and NSC57969, have been identified with increased MDR-selective toxicity (Pape et al., 2022).

Recently, we have discovered MX106 and its analogs, which are designed and synthesized as survivin inhibitors, exhibited potent CS effects killing ABCB1-overexpressing MDR colorectal cancer cells selectively (Xiao et al., 2017). Among those compounds, MX106-4C (5-(((2-bromo-4-methylbenzyl)oxy)methyl)-7-(pyrrolidine-1-ylmethyl)quinolin-8-ol)) (Fig. 1A) has been identified as a leading compound with the most potent selective toxicity against ABCB1-positive colorectal cancer cells.

The core structure of MX106-4C aligns with the pharmacophore of 8-OHQ MDR-selective compounds. The present study aims to investigate the 8-OHQ structure-related mechanisms and the survivin-related on-target mechanisms by which compound MX106-4C selectively kills ABCB1-positive colorectal cancer cells. Furthermore, the efficacy of MX106-4C using co-administrative treatment with anti-cancer drugs or as a re-sensitizing agent in colorectal cancer cells was evaluated.

2. Material and methods

2.1. Chemicals and reagents

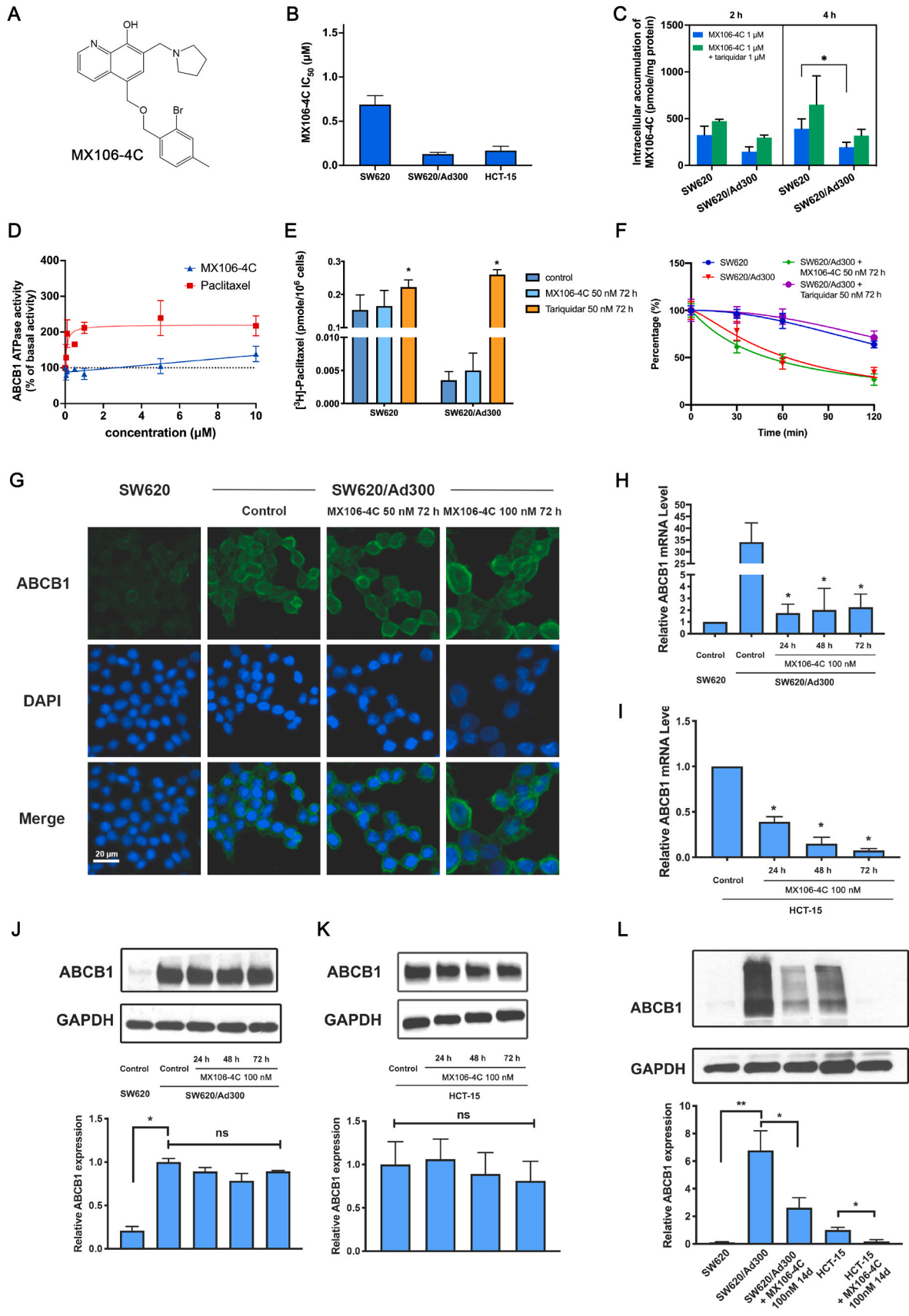
Compound MX106-4C was synthesized and characterized according to our previously reported procedure (Xiao et al., 2019). Dulbecco's modified Eagle's medium (DMEM), fetal bovine serum (FBS), and 0.25% trypsin-EDTA were ordered from Corning Inc. (New York, NY). Eagle's minimum essential medium (EMEM) was purchased from ATCC (American Type Culture Collection, Manassas, VA). Doxorubicin, oxaliplatin, 5 fluorouracil (5-FU), tariquidar, formaldehyde, Triton X-100, 3-(4, 5-dimethylthiazol-yl)-2, 5-diphenyltetrazolium bromide (MTT), agarose, and N-acetylcysteine were purchased from Sigma Chemical Co. (St. Louis, MO). Geneticin (G418) and cisplatin were obtained from Enzo Life Sciences (Farmingdale, NY). The radiolabeled drug [³H]-paclitaxel (31 Ci/mmol) was ordered from Moravek Biochemicals, Inc. (Brea, CA). Annexin V-FITC, annexin-V binding buffer, and PI/RNase staining buffer were purchased from BD Biosciences (San Jose, CA). The antibodies used are listed in Table S1. Other reagents were ordered from Thermo Fisher Scientific Inc. (Rockford, IL).

2.2. Cell lines and cell culture

The human colorectal adenocarcinoma HCT-15 cell line and human adenocarcinoma HeLa S3 cell line (CCL-2.2) were purchased from ATCC (American Type Culture Collection, Manassas, VA). The HeLa S3 cells respectively transduced with WT ABCB1, TM6,12-14 A, and TM6,12-14A-EQ mutants, were generated by BacMam Baculovirus transient transduction as previously described (Sajid et al., 2020). The human colorectal adenocarcinoma SW620 and the derived ABCB1 overexpressing SW620/Ad300 cell lines were kind gifts from Dr. Susan E. Bates (Columbia University, NY) and Dr. Robert W. Robey (NCI, NIH, MD). All the aforementioned cell lines were cultured in 10% FBS-supplemented DMEM with the addition of 100 unit/mL penicillin/streptomycin. The SW620/Ad300 cell line was maintained in a complete culture medium containing 300 ng/mL doxorubicin, which were switched to drug-free medium at least 2 weeks before experiments. The stable ABCB1 gene knockout sublines from SW620/Ad300 and HCT-15, termed SW620/Ad300-ABCB1ko and HCT-15-ABCB1ko, were established using CRISPR/Cas9 technology as previously described (Lei et al., 2021) and cultured in 10% FBS-supplemented DMEM with the addition of selective agent G418 (1.5 mg/mL). The stably transfected cell lines HEK293/pcDNA 3.1 and HEK293/ABCB1, which were gifts from Dr. Robert W. Robey (NCI, NIH, MD), were cultured in 10% FBS-supplemented DMEM with the addition of 2 mg/mL G418. The human normal colorectal fibroblast CCD-18Co cell line was generously given by Dr. Diane Hardej (St. John's University, NY). The CCD-18Co cells were cultured in EMEM supplemented with 10% FBS and 100 unit/mL penicillin/streptomycin. All cell lines were cultured in a 37 °C humidified incubator containing 5% CO₂.

2.3. Cytotoxicity assay and combinational administration studies

The MTT assay was performed to determine the cytotoxicity of compound MX106-4C and other anticancer drugs as described previously (Xiao et al., 2017). The half-maximal inhibitory concentration (IC₅₀) values were calculated from the concentration-response curve to represent the cytotoxicity of the compound. The resistant fold was



(caption on next page)

Fig. 1. Collateral sensitivity of MX106-4 C in ABCB1 overexpressing MDR colorectal cancer cells. (A) Chemical Structure of compound MX106-4 C. (B) Cytotoxicity of compound MX106-4 C on colorectal cancer cells determined by MTT assay. (C) LC-MS/MS detection of intracellular accumulation of MX106-4 C in SW620 and SW620/Ad300 cells after 2 h and 4 h exposure to 1 μ M MX106-4 C with or without the combination of 1 μ M tariquidar. Data were normalized by the protein content of each sample. (D) Effect of compound MX106-4 C on vanadate (Vi)-sensitive ABCB1 ATPase activity depicted as changes in the percentage of basal ATPase activity in response to concentration change. Paclitaxel, as an ABCB1 substrate that can stimulate ABCB1 ATPase activity, was used as a positive control. (E) The intracellular accumulation of [3 H]-paclitaxel in SW620, and SW620/Ad300 after 72 h exposure of vehicle control, 50 nM MX106-4 C or 50 nM tariquidar. * $p < 0.05$ compared to control group. (F) The [3 H]-paclitaxel efflux activities of SW620 and SW620/Ad300 after 72 h exposure to vehicle control, 50 nM MX106-4 C or 50 nM tariquidar. (G) ABCB1 and DAPI fluorescence micrographs were combined to create a merged image. ABCB1 expression was shown in green and cell nuclei were stained blue by DAPI. (H) (I) Effect of short-term (0–72 h) exposure to MX106-4 C on the transcriptional level of ABCB1 in colorectal cancer cells. The mRNA expression levels of the ABCB1 gene are normalized by the expression of the GAPDH gene. Relative mRNA expression was presented as fold change versus SW620 (H) or HCT-15 control (I). * $p < 0.05$ compared to SW620/Ad300 control group (H) or compared to HCT-15 control group (I). (J) (K) ABCB1 protein expression level change after short-term exposure to 100 nM MX106-4 C. GAPDH was the loading control. Relative ABCB1 protein expression was presented as fold change versus SW620/Ad300 control (J) or HCT-15 control (K). (L) ABCB1 protein expression level change after 14-day exposure to 100 nM MX106-4 C. Protein extraction was done at the end of the 14-day incubation. Relative ABCB1 protein expression was presented as fold change versus HCT-15 control. All data represented the mean \pm SD of three independent experiments.

calculated by dividing the IC₅₀ value obtained from the ABCB1 overexpressing cells by that from the parental cell line. Cytotoxicity assays with HeLa S3 cells expressing ABCB1, TM6,12-14 A, or TM6, 12-14A-EQ mutant were conducted by incubating the cells with various concentrations of compound MX106-4 C for 48 h at 37 °C, followed by cell viability test using Cell Titer Glo reagent kit (Promega) as described earlier (Sajid et al., 2020).

In tests involving long-term (14 days) exposure, 50000 cells were seeded into a T25 flask and incubated in the growth medium for 24 h to ensure adherence before starting treatment. During the 14-day treatment, the culture medium was replaced with a fresh medium containing 100 nM MX106-4 C every 2–3 days. Cells were allowed to recover in a drug-free medium after treatment until 70% confluency was reached, then cells were harvested and seeded onto 96-well plates for MTT cytotoxicity assay.

For reversal study, cells were treated with varying concentrations of MX106-4 C, doxorubicin, or cisplatin, with or without adding 1 μ M tariquidar 2 h before the treatment started. MTT assay was conducted at the end of the treatment and the IC₅₀ values of a compound with or without co-administration of tariquidar were compared to measure the reversal effect. For drug combination experiments, cells were co-treated with different concentrations of MX106-4 C, doxorubicin, 5-FU, or oxaliplatin for 72 h. The cell viability was determined by MTT assay, and the inhibitory effect of each combination was measured by the percentage of cell viability reduction compared to the control group. The data was further analyzed using CompuSyn software (ComboSyn Inc, Paramus, NJ). The combination index (CI) was calculated based on the Chou-Talalay method (Chou, 2010).

2.4. Analysis on intracellular accumulation of compound MX106-4 C

SW620 and SW620/Ad300 cells were seeded into 10 cm culture dishes at a density of 5×10^6 cells per dish and cultured for 24 h. Then, cells were incubated with complete growth medium containing vehicle control or 1 μ M compound MX106-4 C for 2 h and 4 h with or without the combination of 1 μ M tariquidar, respectively. After incubation, cells were harvested and washed three times with PBS. The centrifuged cell pellets were lysed in 200 μ L ice-cold methanol (>99%) by vortex-mixing for 2 min followed by centrifuge at 12000 rpm for 4 min. The supernatant was subjected to further preparation for LC-MS/MS analysis, meanwhile, the pellet was dissolved by 1 mL 0.3 M NaOH and subjected to protein quantification using Bradford assay. The intracellular compound concentration was normalized by the pellet protein quantity.

2.5. ABCB1 ATPase assay

The ABCB1 ATPase assay using prepared ABCB1 crude membranes vesicles of High-five insect cells in the presence of compound MX106-4 C or paclitaxel (0 – 10 μ M) was performed as mentioned previously (Ambudkar, 1998; Ji et al., 2019).

2.6. [3 H]-Paclitaxel accumulation and efflux assay

The effect of compound MX106-4 C on the intracellular accumulation and efflux of [3 H]-paclitaxel was determined in SW620 and SW620/Ad300 cells. Cells were incubated at 37 °C in the presence or absence of MX106-4 C (50 nM) or tariquidar (50 nM) for 72 h. At the end of incubation, the cells were harvested, and cell counting was performed. The cell suspensions were diluted to the same density for all groups, followed by an additional 2 h incubation in a medium containing 10 nM [3 H]-paclitaxel with or without MX106-4 C or tariquidar. After incubation, cells were washed with ice-cold PBS and then incubated in a medium free of [3 H]-paclitaxel, with or without MX106-4 C or tariquidar. At various time points (0, 30, 60, 120 min), cells were harvested and transferred into scintillation fluid. The radioactivity was detected using the liquid scintillation counter (Packard Instrument, IL).

2.7. Immunofluorescence assay

SW620 and SW620/Ad300 cells were seeded at a density of 1×10^5 cells on sterilized glass coverslips pretreated with 0.1 mg/mL poly-D-lysine in 6-well plates. After 24 h culturing that enabled the cells to stabilize and attach to the glass coverslip, a 72 h incubation with vehicle control, 50 or 100 nM MX106-4 C was conducted. Thereafter, the cells were prepared and subjected to immunofluorescence staining and imaging was carried out following the procedures described previously (Yang et al., 2020).

2.8. Reverse transcription-quantitative PCR (RT-qPCR)

The total mRNA of cells was extracted using Trizol reagent following the manufacturer's protocol. Reverse transcription was performed for cDNA synthesis. Quantitative gene analysis was performed using the fluorescent dye SYBR Select Master Mix (Applied Biosystems, Foster City, CA). The primer sequences are listed in Table S2. The PCR reactions were conducted in Aria Mx Real-Time PCR System (Agilent Technologies, Santa Clara, CA). The mRNA expression was quantified using the delta-delta Ct method and normalized by the expression of the GAPDH gene.

2.9. Western blotting analysis

Total cell protein extraction and Western blotting analysis were performed as previously described (Liao et al., 2019). Primary and secondary antibodies were diluted as indicated in Table S1 with a blocking agent before application. The blocking agent and antibody diluting agent was 5% non-fat milk in TBST, which was switched to 5% BSA in TBST when phosphorylated protein was detected. The signal was detected using enhanced chemiluminescence.

2.10. Cell apoptosis and cell cycle assay

SW620, SW620/Ad300, and SW620/Ad300-ABCB1ko cells were exposed to 50 nM MX106–4 C for 0, 24, 48, 72 h, or 100 nM MX106–4 C for 72 h. At the end of the exposure period, the apoptotic cells in each group were detected by flow cytometry using BD Pharmingen FITC Annexin V apoptosis detection kit (BD Biosciences, San Jose, CA) following the manufacturer's instruction. Cell cycle analysis was performed using flow cytometry for the harvested cells after treatment, following the previously developed procedure (Narayanan et al., 2019).

2.11. Intracellular reactive oxygen species (ROS) measurement

SW620, SW620/Ad300, and SW620/Ad300-ABCB1ko cells were incubated with 100 nM MX106–4 C for 0, 24, 48, 72 h, or 200 nM MX106–4 C with or without 5 mM N-acetylcysteine for 72 h. Subsequently, cells were harvested, washed with PBS, and incubated with ROS indicator CM-H₂DCFDA (10 μM) in the dark for 30 min at 37 °C. The fluorescent product of CM-H₂DCFDA generated by the action of intracellular peroxides was detected by measuring the fluorescence intensity at excitation wavelength 495 nm and emission wavelength 520 nm using Synergy H1 Hybrid plate reader (BioTek, Winooski, VT). After reading, the samples were lysed for protein quantification using the BCA assay. The fluorescence intensity data were normalized by protein content for each sample.

2.12. Intracellular GSH measurement

SW620, SW620/Ad300, and SW620/Ad300-ABCB1ko cells were incubated with 100 nM MX106–4 C for 0, 24, 48, 72 h, or 200 nM MX106–4 C with or without 5 mM N-acetylcysteine for 72 h. After treatment, cells were harvested using a cell scraper with PBS. The cell pellets were collected by centrifugation and homogenized using cold MES buffer, followed by centrifuge at 10,000 g for 15 min at 4 °C. The supernatant was collected and split into two portions: a half portion was submitted to intracellular GSH detection using Cayman's GSH assay kit (Cayman Chemical Inc., Ann Arbor, MI) according to the manufacturer's protocol; the other half portion was subjected to BCA protein quantification assay for normalization of data.

2.13. Intracellular ATP Measurement

Cells were seeded in 96-well black microplates and were exposed to vehicle control or 50 or 100 nM of MX106–4 C, or a combination of MX106–4 C with 1 μM tariquidar, for 72 h. Then, intracellular ATP concentration was determined using the ATPlite Luminescence Assay System (PerkinElmer) following the manufacturer's instruction. Intracellular ATP levels were detected by luminescence measurement using Synergy H1 Hybrid plate reader. The relative ATP levels of the treated samples were calculated by dividing their ATP levels with those of the control group after data was normalized by total protein.

2.14. Caspases-3/7 assay

SW620, SW620/Ad300, and SW620/Ad300-ABCB1ko cells were exposed to vehicle control or 50 or 100 nM of MX106–4 C, or a combination of MX106–4 C with 1 μM tariquidar, for 72 h. At the end of incubation, cells were harvested and washed with PBS. Then, cells were incubated with CellEvent™ Caspase 3/7 Green Detection Reagent (Invitrogen), and the caspase-3/7 activity was determined by flow-cytometric measurement on the fluorescence product from cleavage of the detection reagent by active caspases-3/7 using BD Accuri C6 flow cytometer (BD, Franklin Lakes, NJ).

2.15. mRNA sequencing analysis

SW620 and SW620/Ad300 cells were treated with vehicle control or 100 nM of MX106–4 C for 72 h. At the end of treatment, the total RNA of each group was extracted using the Rneasy Plus Mini Kit (Qiagen, Hilden, Germany). The purified RNA samples were subjected to cDNA library construction and Illumina NovaSeq 6000 conducted at Novogene Corporation Inc. (Durham, NC, USA). The mRNA profiles were compared between cells incubated with MX106–4 C and vehicle, as well as between SW620 and SW620/Ad300 cells. Differentially expressed genes (DEGs) with a significance level of $p < 0.05$ and fold change > 2 between groups were screened for Kyoto Encyclopedia of Genes and Genomes KEGG pathway enrichment analysis through performed through the online accessible DAVID Bioinformatics Resources 6.8 (NIAID/NIH, <https://david.ncifcrf.gov>). Graphical visualizations of data were carried out using GraphPad Prism 8 software (GraphPad Software, La Jolla, CA) for the volcano plots, and Bioinformatics online platform (<http://www.bioinformatics.com.cn/en>) for cluster heatmaps and enrichment bubble plots.

2.16. Reverse phase protein array (RPPA)

SW620 and SW620/Ad300 cells were treated with vehicle control or 200 nM of MX106–4 C for 72 h. After treatment, total protein lysate was prepared, quantified, and gradiently diluted. The diluted samples were subjected to the RPPA processed by Mills Institute for Personalized Cancer Care, Fynn Biotechnologies Ltd. (Shandong, China). A protein expression file of 307 cancer-related genes was generated for each treatment group. Identification of DEGs and bioinformatic analysis were further carried out.

2.17. Anti-cancer efficacy test in 3D multicellular tumor spheroids (MCTSs)

Cells were seeded into 1% agarose-coated 96-well plates (500 cells/well for SW620, SW620/Ad300, and SW620/Ad300-ABCB1ko cells, 1500 cells/well for HCT-15 and HCT-15-ABCB1ko cells). The MCTSs were treated with 300 nM MX106–4 C at 48 h post-seeding of the cells when the MCTS aggregates formed to approximately 300 to 400 μm in diameter. At time points 0, 24, 48, and 72 h, imaging and measurements were performed as previously described (Lei et al., 2021).

2.18. Statistical analysis

Statistical analysis was carried out in the GraphPad Prism 8 software (GraphPad Software, La Jolla, CA). Comparisons between mean values of multiple groups were carried out using one-way ANOVA and the subsequent Tukey's post hoc test. Dunnett's post hoc test was used after ANOVA when multiple groups were compared with one control group. Comparisons between mean values of HCT-15 cells and HCT-15-ABCB1ko cells were carried out using Student's t-test. A criterion of $p < 0.05$ is set for statistical significance.

3. Results

3.1. Selective toxicity of compound MX106-4C against ABCB1 overexpressing cells

The cytotoxicity of MX106–4 C in colorectal cancer cells was compared with the other ABCB1 substrate anti-cancer drugs, including doxorubicin and survivin-targeted drug YM-155 (Table 1). Although doxorubicin and YM-155 exhibited higher efficacy than MX106–4 C in inhibiting the cell viability of parental cancer cell line SW620, the cytotoxic effects were sharply reduced in MDR cell line SW620/Ad300. In contrast, MX106–4 C showed approximately 10-fold higher potency in ABCB1 overexpressing SW620/Ad300 cells compared to the parental

Table 1

Selective toxicity of compound MX106–4 C against ABCB1 overexpressing and the parental cell lines.

Treatment	IC ₅₀ ± SD ^a (μM)		Fold Resistance ^b
	SW620	SW620/Ad300	
MX106-4 C	0.6755 ± 0.2027	0.0664 ± 0.0462	0.10
YM-155	0.0039 ± 0.0007	23.3681 ± 2.3697	5931.42
doxorubicin	0.1032 ± 0.0164	15.2409 ± 1.8908	147.68
cisplatin	1.7948 ± 0.0571	5.1210 ± 0.6467	2.85
	HEK293/pcDNA3.1	HEK293/ABCB1	
MX106-4 C	0.2426 ± 0.0579	0.0033 ± 0.0006	0.01
YM-155	0.0034 ± 0.0014	47.0512 ± 6.5968	13978.47
doxorubicin	0.0742 ± 0.0106	0.2655 ± 0.0432	3.58
cisplatin	2.2929 ± 0.4799	2.3310 ± 0.4873	1.02

^a IC₅₀: concentration that reduces cell viability by 50% (mean ± SD). Values in the table are determined from at least three independent experiments conducted in triplicate.

^b Fold Resistance represents the IC₅₀ value of the drug from ABCB1 overexpressing cells divided by that from parental cells.

SW620 cells. As a negative control, cisplatin, which is not a substrate of ABCB1, showed similar sensitivity in drug resistant cells and the parental cells. To further confirm the role of ABCB1 overexpression in the selective toxicity of compound MX106–4 C, *ABCB1* gene transfected HEK293/ABCB1 and the vector control HEK293/pcDNA3.1 cells were subjected to cytotoxicity testing. Similar results were observed from HEK293/ABCB1 and HEK293/pcDNA3.1 cells: HEK293/ABCB1 cells were resistant to doxorubicin and YM-155 but not to cisplatin compared to HEK293/pcDNA3.1 cells, and collaterally sensitive to compound MX106–4 C with a fold resistance as low as 0.01 was shown in HEK293/ABCB1 cells. This suggested that ABCB1 was a major factor contributing to the selective toxicity of MX106–4 C in ABCB1 overexpressing MDR cells.

Resistance to chemotherapy mediated by ABCB1 in colorectal cancer can be intrinsic due to endogenous ABCB1 expression. To determine whether compound MX106–4 C has a high inhibitory effect on non-selected ABCB1 positive colorectal cancer cells, the HCT-15 cell line, which is known to have intrinsic overexpression of ABCB1, was tested. The result showed that, compared to SW620 cells with low ABCB1 expression, HCT-15 cells were hypersensitive to MX106–4 C, with an IC₅₀ value as low as 0.167 ± 0.018 μM (Fig. 1B), indicating that MX106–4 C could be useful not only in treating drug-induced ABCB1 positive colorectal cancer, but also in combating colorectal cancer that intrinsically expressed ABCB1.

3.2. Intracellular accumulation levels of MX106-4 C in parental and resistant colorectal cancer cells

To investigate whether the selective toxicity of MX106–4 C is contributed by elevated MX106–4 C concentration in ABCB1 overexpressing cells, the intracellular accumulation of MX106–4 C was determined and compared between SW620 and SW620/Ad300 cells. As shown in Fig. 1C, the amount of MX106–4 C in cells remained at a comparable level with 2 h and 4 h exposure. The intracellular accumulation of MX106–4 C in SW620 cells was slightly higher than that in SW620/Ad300 cells. However, the ABCB1 inhibitor tariquidar did not exert an obvious effect on the accumulation of MX106–4 C. This indicated that the intracellular level of compound MX106–4 C may not be affected by ABCB1. The higher toxicity of MX106–4 C in ABCB1 overexpressing SW620/Ad300 cells was not likely to be associated with ABCB1-dependent uptake or efflux of the compound.

3.3. Interaction of MX106-4 C and ABCB1 in colorectal cancer cells

The effect of compound MX106–4 C on the function of ABCB1 was investigated by ABCB1 ATPase assay and [³H]-paclitaxel accumulation

and efflux assay. Unlike paclitaxel, which is an ABCB1 substrate that can stimulate ABCB1 ATPase activity, compound MX106–4 C at up to 10 μM did not have a significant effect on ABCB1 ATPase activity (Fig. 1D), confirming that MX106–4 C is not likely to be a substrate of ABCB1. Furthermore, this result suggested that the collateral sensitivity of MX106–4 C was not through disturbing the ATP hydrolysis function of ABCB1. Consistent with the observation that MX106–4 C neither inhibited nor stimulated ABCB1 ATPase, MX106–4 C did not have significant effects on the efflux function of ABCB1. After exposure to 50 nM of MX106–4 C for 72 h, the intracellular [³H]-paclitaxel level remained at approximately the same level as the corresponding control group for SW620 and SW620/Ad300 cells, respectively (Fig. 1E). The low retention of [³H]-paclitaxel due to ABCB1 exporting activity in SW620/Ad300 cells was not significantly affected by MX106–4 C (Fig. 1F). On the contrary, the ABCB1 inhibitor tariquidar, at the same concentration of 50 nM, could significantly increase the intracellular accumulation and then decelerate the efflux of [³H]-paclitaxel in SW620/Ad300 cells. The [³H]-paclitaxel accumulation in SW620 cells was also elevated by tariquidar to a small extent, possibly due to the inhibitory effect on the endogenous ABCB1 in SW620 cells. As indicated by the negative results observed from the MX106–4 C-treated group compared to the tariquidar-treated group, compound MX106–4 C may not be a functional inhibitor of ABCB1.

Since the function of ABCB1 was not affected by compound MX106–4 C, the selective toxicity may be related to the change of the subcellular localization or the expression of ABCB1. Therefore, the immunofluorescence assay was performed to investigate the effect of compound MX106–4 C on the distribution of ABCB1 expression in cells. As illustrated in Fig. 1G, the overexpression of ABCB1 on the plasma membrane in SW620/Ad300 cells was confirmed by the higher green fluorescence intensity compared to the parental SW620 cells. After 72 h exposure to 50 nM of MX106–4 C, the subcellular localization of ABCB1 was not significantly altered, which remained majorly on the cell membrane. A higher concentration of MX106–4 C at 100 nM exerted more observable toxicity to SW620/Ad300 cells as indicated by the cell swelling phenomenon, however, the ABCB1 expression (fluorescence intensity) and subcellular localization did not show obvious change compared to the low concentration group and control group.

The effect of compound MX106–4 C on the expression of ABCB1 in colorectal cancer cells at the transcriptional level as well as protein level was further determined. As demonstrated in Fig. 1H, from 24 h to 72 h, MX106–4 C at 100 nM significantly downregulated ABCB1 mRNA level in SW620/Ad300 cells to a level comparable to the parental SW620 cells. A similar result was observed from HCT-15 cells. The down-regulating effect of MX106–4 C on ABCB1 mRNA level was time-dependent in HCT-15 cells (Fig. 1I) whereas this time-dependent pattern was not obvious in SW620/Ad300 cells. Albeit a significant reduction in ABCB1 mRNA level was induced by MX106–4 C, the protein expression of ABCB1 was almost unchanged in MX106–4 C-treated SW620/Ad300 and HCT-15 cells (Figs. 1J and 1K). Considering that change in protein expression level may require a longer time to be observable after transcriptional alternation, the ABCB1 protein level was determined in SW620/Ad300 and HCT-15 cells after extended exposure to compound MX106–4 C for up to 14 days. After long-term treatment, the ABCB1 protein expression was significantly downregulated in SW620/Ad300 and HCT-15 cells (Fig. 1L). As the transcriptional activity but not the function and expression of ABCB1 was not affected by MX106–4 C in short-term exposure, and change in ABCB1 protein expression required prolonged exposure, MX106–4 C may have an indirect regulatory effect on ABCB1 instead of direct interaction. The result from cellular thermal shift assay further confirmed the hypothesis that MX106–4 C does not have a direct interaction with ABCB1 (Fig. S1).

3.4. Association between the selective toxicity of MX106-4 C with ABCB1 expression and function

To verify the role of ABCB1 expression in MX106-4 C-induced selective toxicity, the ABCB1 gene knockout sublines of SW620/Ad300 and HCT-15 cell lines were tested. The knockout of ABCB1 was verified using Western blotting (Figs. S2A and S2B). It was observed that ABCB1 gene knockout re-sensitized SW620/Ad300 and HCT-15 cells to ABCB1 substrate drug doxorubicin, while the response to non-substrate drug cisplatin was unaffected (Figs. 2B and 2C). Conversely, the sensitivity of SW620/Ad300 and HCT-15 cells to MX106-4 C was significantly reduced (Fig. 2A). The SW620/Ad300-ABCB1ko cells were even more unresponsive to MX106-4 C compared to SW620 cells, possibly due to the endogenous ABCB1 expression in SW620. These results inferred that the collateral sensitivity effect induced by MX106-4 C is ABCB1 expression-dependent.

As the dependence of MX106-4 C selective toxicity on ABCB1 expression has been suggested, whether this selective toxicity requires functional ABCB1 was investigated. Tariquidar was used to inhibit the ABCB1 efflux function in cytotoxicity tests with MX106-4 C. To exclude the possible direct toxic effect from tariquidar, the selected concentration 1 μ M for tariquidar had been confirmed to be non-toxic and effective in inhibiting ABCB1 function in preliminary tests before reversal study was performed (data not shown). As expected, inhibition of ABCB1 using tariquidar resulted in an effective reverse of doxorubicin resistance in SW620/Ad300 cells (Fig. 2E) and HCT-15 cells (Fig. 2H), while the IC₅₀ values of cisplatin remained approximately the same (Figs. 2F and 2I). With ABCB1 function blocked by tariquidar, SW620, SW620/Ad300, and HCT-15 cells became significantly less sensitive to MX106-4 C (Figs. 2D and 2G), suggesting that functional ABCB1 was necessary for compound MX106-4 C to induce selective toxicity.

The roles of ABCB1 efflux function and ATP hydrolysis function in selective toxicity of MX106-4 C were further examined respectively using HeLa S3 cells expressing wild-type (WT) ABCB1, TM6,12-14 A mutant ABCB1 with impaired efflux and acquired uptake function, and TM6,12-14A-EQ mutant ABCB1 with deficient ATPase function (Sajid et al., 2020). The ABCB1 expression and altered ABCB1 function in these cell lines were confirmed by immunofluorescence and Rhodamine123 transporting assay (Figs. S2C and S2D). The untransduced HeLa S3 cells without ABCB1 expression were used as a control. The results showed that the TM6,12-14 A mutant was less sensitive to MX106-4 C compared to cells with WT ABCB1, whereas the TM6,12-14A-EQ mutant was even more irresponsive with an IC₅₀ value comparable to the untransduced cells (Figs. 2J and 2K). This suggested that the hypersensitivity to compound MX106-4 C is dependent on the drug efflux activity of ABCB1 and is more critically dependent on the ATPase activity of ABCB1.

3.5. Effect of MX106-4 C on cell apoptosis and cell cycle in ABCB1 positive colorectal cancer cells

As a survivin inhibitor, compound MX106-4 C may affect cell apoptosis or cause cell cycle arrest by inhibiting survivin. To investigate whether the selective toxicity of compound MX106-4 C is correlated to survivin inhibition, the cell apoptosis, cell cycle, survivin expression, and the downstream effector caspases-3/7, were assessed in MX106-4 C-treated colorectal cancer cells.

As shown in Figs. 3A and 3B, compound MX106-4 C increased the rate of apoptosis in ABCB1 overexpressing SW620/Ad300 cells in a concentration-dependent manner; however, this effect was abolished by knocking out the ABCB1 gene from SW620/Ad300 cells. There was also a decrease in the percentage of viable cells with the treatment of compound MX106-4 C in SW620 cells compared to the control group, but not as severe as in SW620/Ad300 cells. These results revealed that MX106-4 C selectively induced apoptosis in ABCB1-positive colorectal cancer cells in dependence on the ABCB1 expression level. It was also

shown that compound MX106-4 C induced G0/G1 phase arrests and reduced population at G2/M phase in SW620/Ad300 cells at 50 nM 48 h and 100 nM 72 h (Figs. 3C and 3D). Interestingly, opposite effects were observed in MX106-4 C-treated SW620 cells compared to the MDR cells. Accumulation at the G2/M phase and decreased population at G0/G1 phase were found in SW620 cells after exposure to MX106-4 C. In addition, when comparing the control groups, SW620 cells had more cell population at the G2/M phase and less cell population at G0/G1 phase than SW620/Ad300 cells, while SW620/Ad300-ABCB1ko cells appeared to be more resemble that of SW620/Ad300 cells. This indicated that there may be differential expressed genes between SW620 and SW620/Ad300 cells related to cell cycle regulation, and those are not regulated by ABCB1 so the SW620/Ad300-ABCB1ko cells remain the same cell cycle phase distribution pattern.

To further investigate whether the cell cycle arrest and apoptosis induced by compound MX106-4 C is correlated to repression on survivin expression in colorectal cancer cells, the transcriptional level, as well as protein level of survivin in MX106-4 C-treated colorectal cancer cells, were determined. As demonstrated in Fig. 3G, MX106-4 C did not alter the mRNA level of survivin but could slightly downregulate survivin protein expression after 72 h treatment (Figs. 3E and 3F). As the down regulation of protein expression is not significant, compound MX106-4 C may have an inhibitory effect on survivin rather than an influence on the expression level. Furthermore, the caspases-3/7 assay results exhibited that compound MX106-4 C increased cleaved caspases-3/7 in ABCB1 overexpressing SW620/Ad300 cells but not in parental SW620 cells or ABCB1 deficient SW620/Ad300-ABCB1ko cells (Fig. 3H). In addition, the combination of compound MX106-4 C with ABCB1 inhibitor tariquidar significantly reduced the activation of caspases-3/7 in SW620/Ad300 cells, while the active caspases-3/7 levels in SW620 cells and SW620/Ad300-ABCB1ko cells were unaffected, suggesting that the cell apoptosis caused by MX106-4 C in SW620/Ad300 cells may be through activation of caspases-3/7, which could be an ABCB1-dependent event.

3.6. Oxidative stress induced by MX106-4 C in colorectal cancer cells

As ROS production and oxidative stress have been considered as a mechanism for CS effects (Pluchino et al., 2012), the intracellular ROS levels and GSH levels were detected in colorectal cancer cells treated with MX106-4 C. Increased intracellular ROS levels and reduced GSH levels were observed in ABCB1 overexpressing SW620/Ad300 cells treated with compound MX106-4 C, following a time-dependent manner (ROS and GSH) and a concentration-dependent manner (GSH) (Figs. 4B and 4D). In SW620/Ad300 cells, the intracellular GSH level reduced by MX106-4 C could be replenished by the addition of 5 mM N-acetylcysteine (NAC), a precursor of GSH acting as ROS scavenger, but the elevated intracellular ROS levels by MX106-4 C were partially reversed. These phenomena were only presented in ABCB1 overexpressing SW620/Ad300 cells but not the parental SW620 or ABCB1 deficient SW620/Ad300-ABCB1ko cells (Fig. 4A-4C), indicating that compound MX106-4 C can selectively lead to oxidative stress in ABCB1 overexpressing cells, which could be partially mitigated by the addition of antioxidant NAC.

Given that compound MX106-4 C could induce oxidative stress on ABCB1 overexpressing cells, which could be mitigated by antioxidant NAC, the ability of NAC to counteract MX106-4 C-induced cytotoxicity and cell apoptosis was then evaluated. The result showed that NAC cannot alleviate the cytotoxicity of compound MX106-4 C on ABCB1 overexpressing SW620/Ad300 cells (Fig. 4H). In addition, the combination of compound MX106-4 C and NAC had no significant difference in cell apoptosis compared to MX106-4 C alone (Fig. 4G), suggesting that compound MX106-4 C-mediated oxidative stress may not be the main mechanism of the CS effect. Since the CS effect of MX106-4 C was found to rely on the ATP hydrolysis activity of ABCB1, the oxidative stress induced by MX106-4 C may be a secondary outcome of ATP

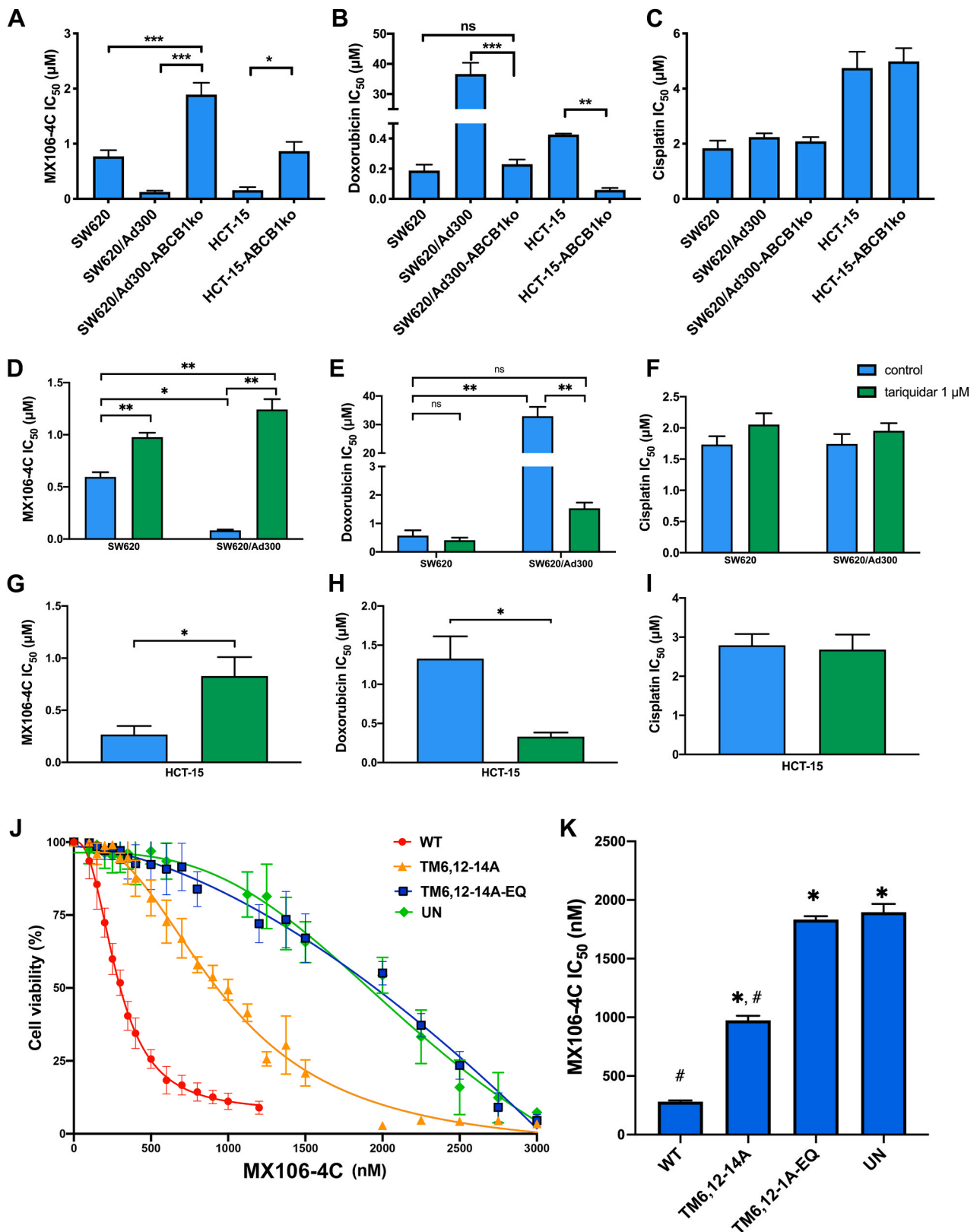


Fig. 2. The role of ABCB1 expression and function in the selective toxicity of MX106-4 C. (A)-(C) The IC₅₀ values of MX106-4 C, doxorubicin, and cisplatin in SW620/Ad300 and HCT-15 cells were determined by MTT assay. Columns and error bars represented mean \pm SD of IC₅₀ values acquired from three independent experiments in triplicate. (D)-(I) Reversal effects of tariquidar on drug sensitivities of colorectal cancer cells to MX106-4 C, doxorubicin, and cisplatin. Columns and error bars represented mean \pm SD of IC₅₀ values acquired from three independent experiments in triplicate. * $p < 0.05$, ** $p < 0.01$, *** $p < 0.001$. (J) (K) Cytotoxicity of compound MX106-4 C compound in untransduced HeLa S3 cells and HeLa S3 cells expressing wild-type (WT), TM6,12-14A, or TM6,12-14A-EQ mutant ABCB1. Data points with error bars displayed the average viability (%) \pm SD obtained from at least three independent experiments performed in triplicate. * $p < 0.05$ compared to WT, # $p < 0.05$ compared to UN.

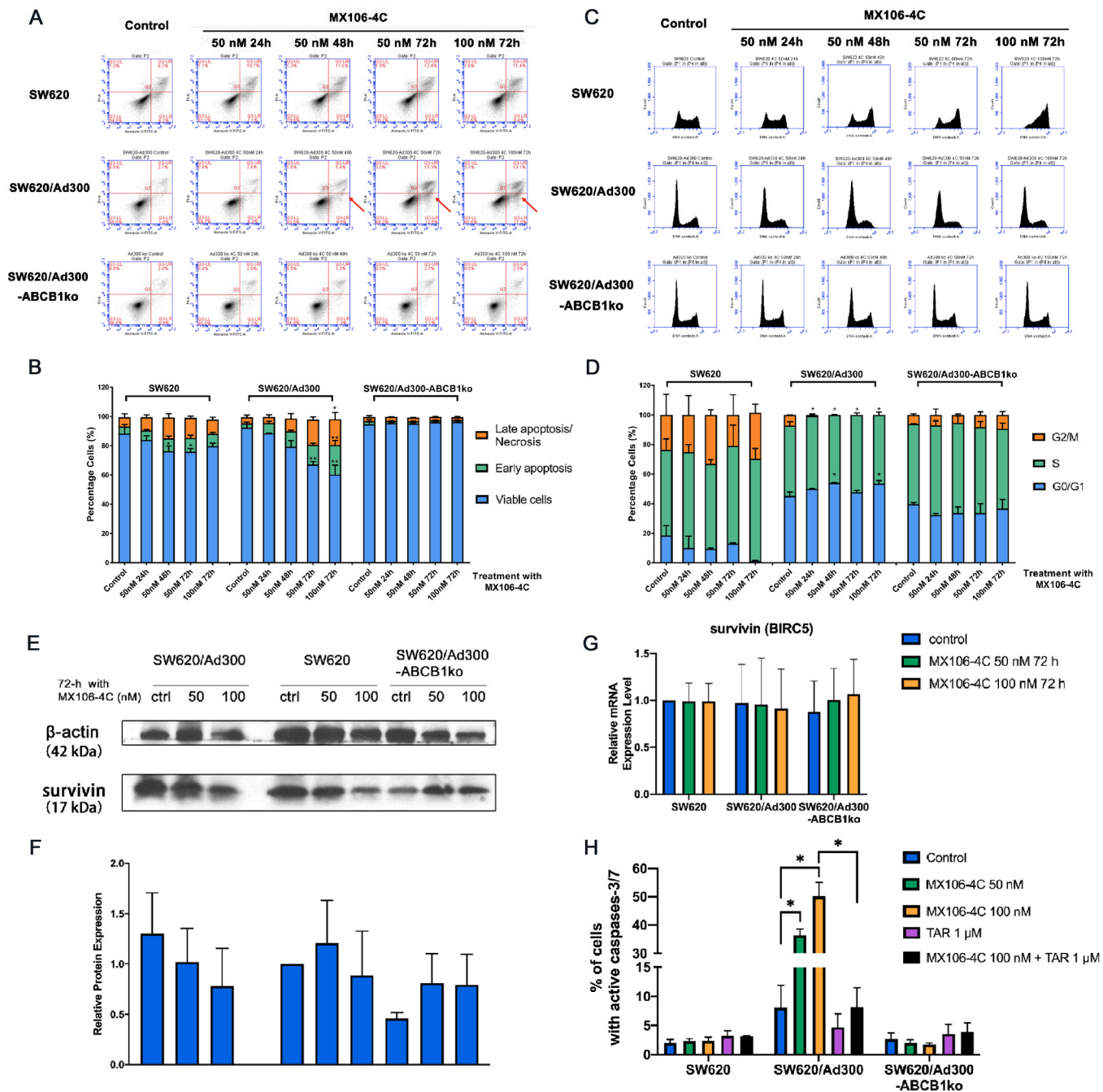


Fig. 3. Effect of MX106-4 C on cell apoptosis, cell cycle, and survivin expression. (A)–(D) Effect of MX106-4 C on cell apoptosis (A) (B) and cell cycle (C) (D) in SW620, SW620/Ad300, and SW620/Ad300-ABC1ko cells. Representative scatter plots of cell apoptosis analysis by PI (y-axis) vs FITC-annexin V (x-axis). Cells were classified as viable cells (Annexin V⁻, PI⁻), early apoptotic cells (Annexin V⁺, PI⁻), late apoptotic/necrotic cells (Annexin V⁺, PI⁺), and damaged cells (Annexin V⁻, PI⁺). The bar graph represented the percentage of cell population at each category. Columns and error bars represent the average cell population (%) and the SD obtained from three independent experiments. * $p < 0.05$ and ** $p < 0.01$ compared to the control group. (E) Western blotting results of survivin protein expression level change after short-term exposure to 100 nM MX106-4 C. β -actin was used as a loading control. (F) Relative survivin protein expression was presented as fold change versus SW620 control. (G) The mRNA expression levels of survivin (*BIRC5* gene) in SW620, SW620/Ad300, and SW620/Ad300-ABC1ko cells after treatment with MX106-4 C. Relative mRNA expression was presented as fold change versus SW620 control (ctrl) group after normalized by the expression of the *GAPDH* gene. (H) The ABCB1-dependent effect of compound MX106-4 C on activating caspases-3/7 in ABCB1 overexpressing SW620/Ad300 cells. The bar graph represented the percentage of cell population with active caspases-3/7 detections. * $p < 0.05$. All columns/data points and error bars represented average values and SD obtained from three independent measurements.

depletion caused by the intensified ATP consumption in ABCB1 overexpressing cells. This hypothesis was further tested by the measurement of intracellular ATP levels. As shown in Figs. 4E and 4F, the ABCB1 overexpressing SW620/Ad300 cells exhibited a relatively lower basal intracellular ATP level compared to the parental SW620 cells and

SW620/Ad300-ABC1ko cells, which may be associated with the higher ATP consumption by overexpressed ABCB1. MX106-4 C significantly decreased intracellular ATP levels by a concentration-dependent order in SW620/Ad300 cells, which can be reversed by ABCB1 inhibitor tariquidar. A similar but less significant effect was observed in SW620 cells

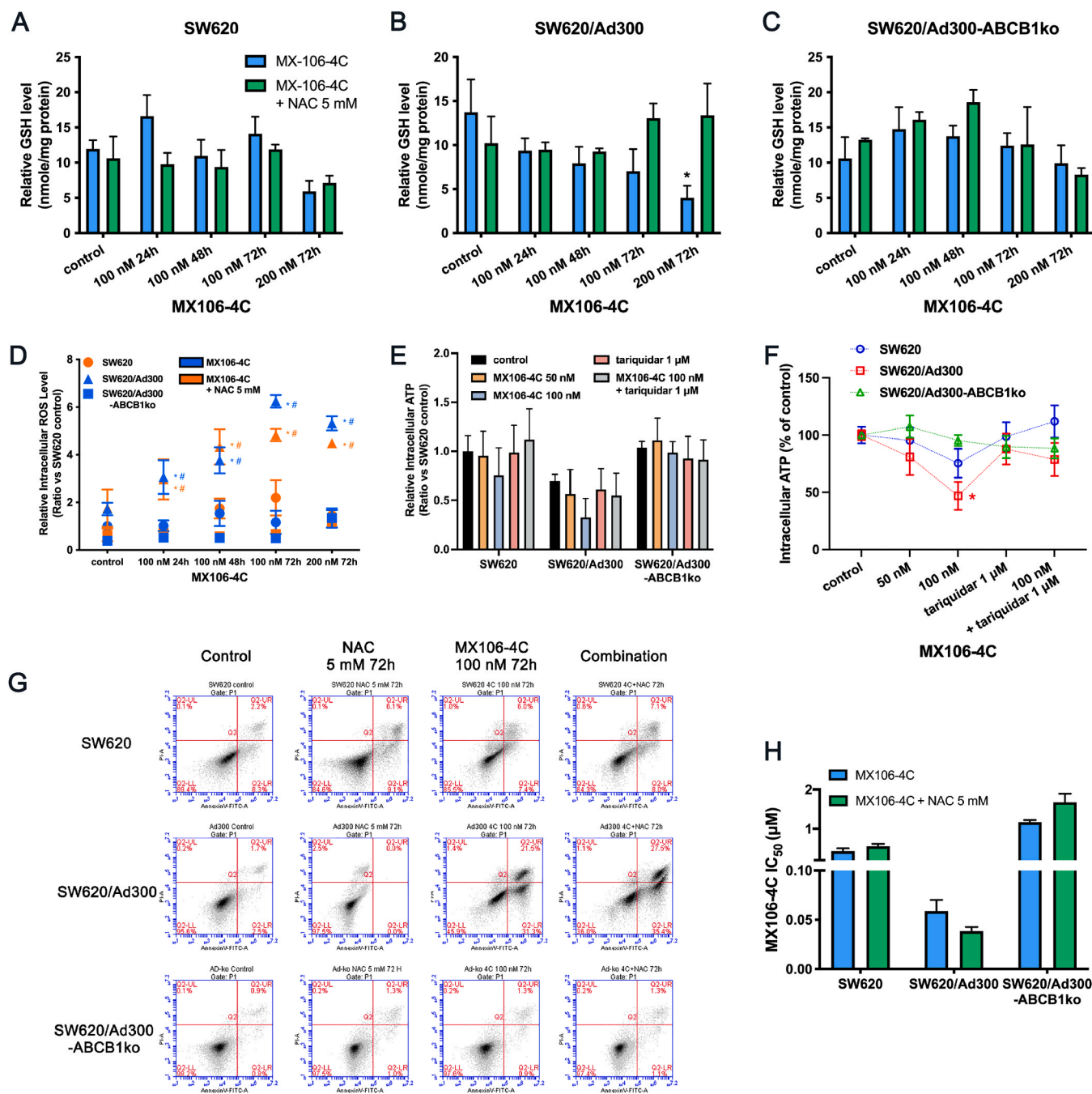


Fig. 4. Effect of MX106-4 C on oxidative stress and intracellular ATP level. (A)-(C) The relative intracellular GSH levels upon treatment of MX106-4 C. * $p < 0.05$ compared to the control group. Relative intracellular ROS levels and relative intracellular GSH levels were calculated by normalizing the ROS (fluorescence intensity) and GSH detection (quantified nmole GSH according to standard curve) data using the protein content of each sample. (D) The relative intracellular ROS levels upon treatment of MX106-4 C with or without NAC. # $p < 0.05$ compared to the control group of the corresponding cell line. * $p < 0.05$ compared to the same treatment of the parental SW620 cell line. (E) The relative intracellular ATP level upon treatment of MX106-4 C, tariquidar, or the combination. The control group of SW620 was used to normalize the other groups. (F) The relative intracellular ATP percentage compared to the untreated control group of each cell lines upon treatment of MX106-4 C, tariquidar, or the combination. * $p < 0.05$ compared to control group. (G) Representative scatter plots of cell apoptosis analysis. (H) The IC₅₀ values of compound MX106-4 C with or without the presence of NAC were determined by MTT assay. All columns/data points and error bars represented average values and SD obtained from three independent measurements.

that express low level of ABCB1, whereas in SW620/Ad300-ABCB1ko cells, the intracellular ATP levels remained relatively unaffected by the treatments. These results suggested that MX106-4 C could induce ABCB1-dependent ATP depletion in MDR colorectal cancer cells, which may be a factor leading to oxidative stress and cell apoptosis.

3.7. Analysis of transcriptionally dysregulated gene expressions induced by MX106-4 C in ABCB1 overexpressing colorectal cancer cells

From mRNA-sequencing analysis, differentially expressed genes (DEGs) with statistical significance were selected with $p < 0.05$, adjust p value (adj p) < 0.05 and fold change > 2 or < 0.5 . Following this criterion, 3079 DEGs were found when comparing SW620/Ad300 control

and SW620 control groups, in which 1389 were upregulated and 1699 were downregulated (Fig. 5A). The DEG with the largest fold change is ABCB1, which showed approximately 123.7-fold upregulated in SW620/Ad300 control group compared to the SW620 control group, which confirmed that the tested samples were reliably reflecting the

ABCB1 expression difference between parental and resistant cells. Most DEGs were upregulated when comparing SW620/Ad300 MX106-4 C group to SW620/Ad300 control group (Fig. 5B), while downregulation of genes was more predominant when comparing SW620 MX106-4 C group to its control group (Fig. 5C). As a result, most of the DEGs (1704

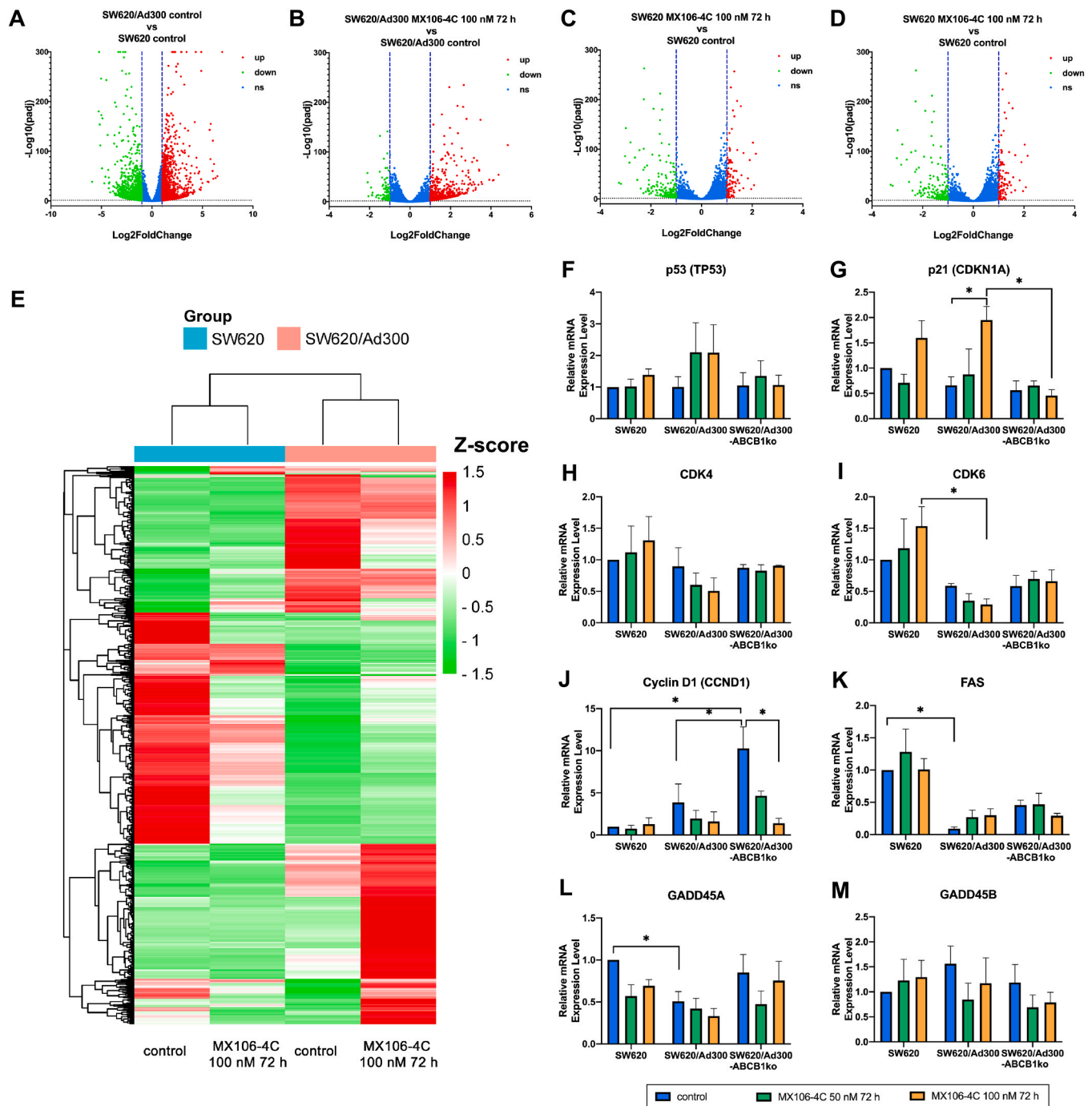


Fig. 5. Differentially expressed genes (DEGs) profile by mRNA-sequencing and validation of mRNA-sequencing data by RT-qPCR. (A)-(D) The volcano scatter plots presented differentially expressed genes between different compared groups: SW620/Ad300 control vs SW620 control (A), SW620 MX106-4 C 100 nM 72 h vs SW620/Ad300 control (B), SW620 MX106-4 C 100 nM 72 h vs SW620 control (C), and SW620 MX106-4 C 100 nM 72 h vs SW620 control (D). padj is the adjusted p value. $\text{Log}_2(\text{Fold Change})$ at -1 and 1 , $-\text{Log}_{10}(\text{padj})$ at 1.3 were labeled by the dotted lines. Differentially expressed genes with $\text{Log}_2(\text{Fold Change}) > 1$ or < -1 and $-\text{Log}_{10}(\text{padj}) > 1.3$ were selected as significant DEGs for heatmap graphing. (E) Heatmap for significantly DEGs. Heatmap is generated based on the fragments per kilobase of transcript per million mapped reads (FPKM) of each gene, which represent the relative expression of the transcript. $Z\text{-score} = (\text{FPKM} - \text{row mean FPKM})/\text{SD}$. (F)-(M) SW620, SW620/Ad300, and SW620/Ad300-ABCB1ko cells were treated with vehicle control, 50 and 100 nM of MX106-4 C, respectively for 72 h. The mRNA expression levels were determined using RT-qPCR. Relative mRNA expression was presented as fold change versus SW620 control group after normalized by the expression of the *GAPDH* gene. Columns and error bars represented average values and standard deviation obtained from at least three independent measurements. * $p < 0.05$.

out of 2008) showed higher expression in SW620/Ad300 MX106-4 C group than SW620 MX106-4 C group (Fig. 5D). The significant DEGs were subjected to heat map graphing for comparison among four groups. The heat map of DEGs revealed that most genes that were upregulated by MX106-4 C treatment in SW620/Ad300 cells did not change in the same trend in SW620 cells (Fig. 5E). This difference might be contributed by the stronger stress induction induced by MX106-4 C in ABCB1 overexpressing SW620/Ad300 cells, or by the altered gene expression profile of SW620/Ad300 cells compared to the parental SW620 cells.

KEGG pathway analysis for DEGs was used to elucidate the pathways related to the gene regulation induced by MX106-4 C. The DEGs between SW620/Ad300 MX106-4 C group and SW620/Ad300 control group did not get any enriched pathway with $\text{padj} < 0.05$ (Fig. S3A). On the other hand, both DEG lists from SW620/Ad300 vs SW620 and SW620 MX106-4 C vs SW620 control got only one significantly enriched pathway in the category of KEGG, which is the p53 signaling pathway (Figs. S3B, S3C). The p53 pathway is closely associated with cell apoptosis and cell cycle regulation. Therefore, dysregulation of the p53 pathway induced by MX106-4 C may be an important mechanism accounting for the selective toxicity of MX106-4 C. The key DEGs that are involved in the p53 pathway were then summarized in Table S3. The trend of expression level changes for the listed gene was validated using RT-qPCR and further tested in SW620/Ad300-ABCB1ko cells to confirm whether the dysregulation of expression induced by MX106-4 C is ABCB1-dependent.

RT-qPCR validation test results showed that *TP53* mRNA levels were comparable among SW620, SW620/Ad300, and SW620/Ad300-ABCB1ko cells (Fig. 5F). The downstream *GADD45A* gene expression was low in SW620/Ad300 compared to parental SW620 and SW620/Ad300-ABCB1ko cells, however, the down regulating trend upon treatment with MX106-4 C was similar among three cell lines (Fig. 5L), which is consistent with the sequencing data. Another downstream molecule of p53, *GADD45B*, was shown slightly upregulated at mRNA level in SW620/Ad300 cells, which was downregulated as SW620/Ad300 cells were exposed to MX106-4 C (Fig. 5M). Since this was inconsistent with the mRNA-sequencing result, and the change was insignificant, it was considered that *GADD45B* mRNA expression may not be affected significantly by MX106-4 C. As *TP53* appeared to be unaffected, whereas the regulation on *GADD45A* was ABCB1-independent, p53 and the downstream *GADD45A* and *GADD45B* may not be majorly involving factors in the MX106-4 C-induced CS effect. *CNKN1A* (p21) was upregulated, and CDK4, as well as CDK6, were downregulated specifically in SW620/Ad300 cells (Fig. 5G-5I), which were consistent with the sequencing data. The cell cycle arrest at G0/G1 induced by compound MX106-4 C may be explained by the dysregulation of the p21-CDK4/CDK6 pathway via a mechanism independent of p53. Unexpectedly, the encoding gene for cyclin D1, *CCND1*, showed a high basal expression in SW620/Ad300-ABCB1ko cells, which was significantly reduced by MX106-4 C (Fig. 5J). As the cell cycle was not shown to be disturbed by MX106-4 C in SW620/Ad300-ABCB1ko cells, further protein level determination is required to investigate this inconsistency. Similar to what was found from mRNA-sequencing data, *FAS* gene expression was low in SW620/Ad300 cells and was approximately 2-fold upregulated upon exposure to MX106-4 C, while the changes in SW620 and SW620-ABCB1ko cells were not obvious (Fig. 5K). Thus, the upregulation of *FAS* might be involved in MX106-4 C apoptosis in SW620/Ad300 cells. However, the transcriptional level may not necessarily reflect the protein expression level, therefore, further validation of protein expression is required.

3.8. Analysis of dysregulated protein expression induced by MX106-4 C in ABCB1 overexpressing colorectal cancer cells

Reverse phase protein array (RPPA) was performed to analyze the dysregulated protein expression induced by MX106-4 C in ABCB1 overexpressing colorectal cancer cells and to identify the potential

mechanism of action. Similar to what was observed from mRNA-sequencing data, the differentially expressed proteins in SW620/Ad300 MX106-4 C group compared to SW620/Ad300 control mostly had an opposite regulatory pattern to the change induced by MX106-4 C in SW620 cells (Fig. 6A, Fig. S4). Proteins that were upregulated upon MX106-4 C treatment in SW620/Ad300 cells were mostly unaffected or downregulated upon MX106-4 C treatment in SW620 cells. The different gene expression profiles between SW620/Ad300 cells and parental SW620 cells may play an important role in causing the differential response to MX106-4 C. Besides, cleaved caspase-3, which is the active form of caspase-3 that mediates cell apoptosis, was shown to be selectively increased in MX106-4 C-treated SW620/Ad300 cells. This confirmed the previous finding from the cell apoptosis assay and caspases-3/7 assay that MX106-4 C could induce cell apoptosis in ABCB1 overexpressing SW620/Ad300 cells via activating caspases-3.

The differentially expressed proteins ($\text{padj} < 0.05$ with fold change > 2 or < 0.5) were further subjected to KEGG pathway analysis. The analysis result showed that the p53 pathway was significantly enriched (Fig. 6B), which suggested that the p53 pathway may be involved in MX106-4 C induced gene dysregulation at the transcriptional level as well as protein level. The differentially expressed proteins that are members in the p53 pathway, including all that got $p < 0.05$ with or without > 2 -fold change, were then summarized in Table S4. And the trend of expression level change induced by MX106-4 C was validated using Western blotting for the listed proteins.

As the RPPA only detects 307 cancer-associated proteins and some hits from mRNA-sequencing may not be included in the list, and to further elucidate the involvement of the p53 pathway in MX106-4 C-induced selective toxicity, protein levels of CDK4 and CDK6 were also detected. As exhibited in Fig. 6C, The Western blotting validation tests results showed that p53, p21, and pRb protein levels were not significantly changed among the cell lines and treatment groups. CDK6 and phospho-pRb proteins were selectively downregulated in ABCB1 overexpressing SW620/Ad300 cells, which was consistent with the RT-qPCR result and the RPPA report, respectively. CDK4 was also downregulated but the effect was not specific to ABCB1 overexpressing cells. Therefore, the selective down regulation of CDK6 and phospho-pRb may explain the selective induction on cell cycle arrest and cell apoptosis by MX106-4 C in ABCB1 positive colorectal cancer cells.

3.9. Synergistic effect of anticancer drugs co-administrated with MX106-4 C on inhibiting colorectal cancer cell viability

The combined cytotoxic effects of MX106-4 C co-administrated with typical ABCB1 substrate doxorubicin, or other chemotherapeutic drugs for colorectal cancer, including 5-FU and oxaliplatin, were assessed in SW620, SW620/Ad300, and HCT-15 cell lines. As the sensitivities to doxorubicin, 5-FU, oxaliplatin, and MX106-4 C are different among the cell lines, the concentrations of doxorubicin, 5-FU, oxaliplatin, and MX106-4 C were adjusted for each cell line by putting the concentration around IC_{50} of single-drug treatment as the median. As shown in Fig. 7A, in SW620 cells, the combinations with CI values < 1 were mostly observed when doxorubicin concentration was 0.03 or 0.1 μM and MX106-4 C concentration was 0.3 or 1 μM , while other combinations had CI values > 1 or closed to 1. This suggested that combination effects were concentration-dependent. On the other hand, in ABCB1 overexpressing SW620/Ad300 and HCT-15 cells, most CI values of the combination were less than 1 except for several closed to 1 (Figs. 7B and 7C), indicating that the cytotoxic effects of doxorubicin in combination with MX106-4 C at the tested concentration ranges could be synergistic in SW620/Ad300 and HCT-15 cells. The difference between SW620 and the other two ABCB1 overexpressing cell lines revealed that MX106-4 C may be beneficial to combat ABCB1-mediated MDR by combination treatment with doxorubicin. Consistent with the results of doxorubicin, 5-FU, which is also a substrate of ABCB1 (Figs. S5C and S5D), had a similar synergistic effect combined with MX106-4 C in SW620/Ad300

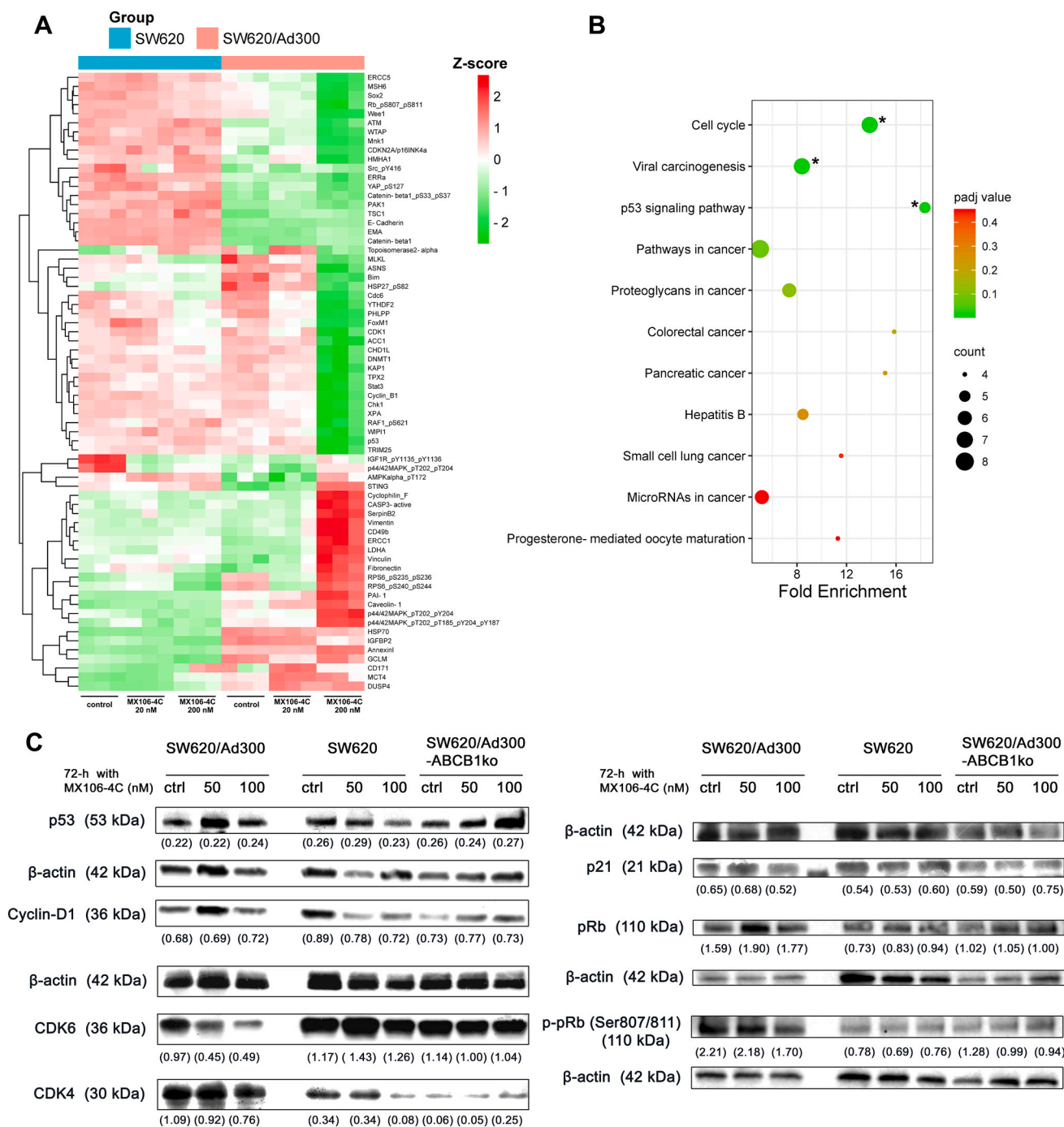


Fig. 6. Differentially expressed protein profile and enrichment analysis by RPPA. (A) Heatmap showed significantly differentially expressed proteins (fold change >2 or <-2 , and $padj < 0.05$) with the name of entry at each row. Heatmap is generated based on normalized \log_2 quantified protein expression values (NormLog2). $Z\text{-score} = \text{NormLog2} - \text{row median NormLog2}$. (B) KEGG pathway enrichment analysis of significantly differentially expressed proteins from RPPA analysis for SW620/Ad300 MX106-4 C 200 nM 72 h vs SW620/Ad300 control comparison. An adjusted p value ($padj$) was obtained by the Bonferroni Sidak method as the false discovery rate. The fold enrichment is the ratio of (number of input genes involved in this pathway/number of all input genes)/(number of genes within this KEGG term on the background list/number of genes on the background list). * $padj < 0.05$. (C) Validation of protein expression by Western blotting. Relative greyscale values were shown below each band, which were determined by the greyscale of the band normalized by the greyscale of the β -actin band on the same PVDF membrane. The greyscale measurements were carried out in ImageJ.

(Fig. S5I) and HCT-15 (Fig. S5J) cells. However, this effect was absent in the parental SW620 cell line (Fig. S5H). Notably, the synergistic effect from the combination of MX106-4 C and oxaliplatin (Figs. S6E-S6G), a non-ABCB1 substrates (Fig. S6A and S6B), were observed in all three cell lines, which indicated the potential of MX106-4 C to synergistically act with anticancer drugs by a mechanism irrelevant to the ABCB1 overexpression.

3.10. Exploiting the CS effect of MX106-4 C to re-sensitize ABCB1 overexpressing MDR colorectal cancer cells

As significant down regulation of ABCB1 had been observed after 14-day exposure to compound MX106-4 C, the alteration on drug sensitivities was further examined to evaluate the capability of compound MX106-4 C to re-sensitize MDR colorectal cancer cells. After 14-day

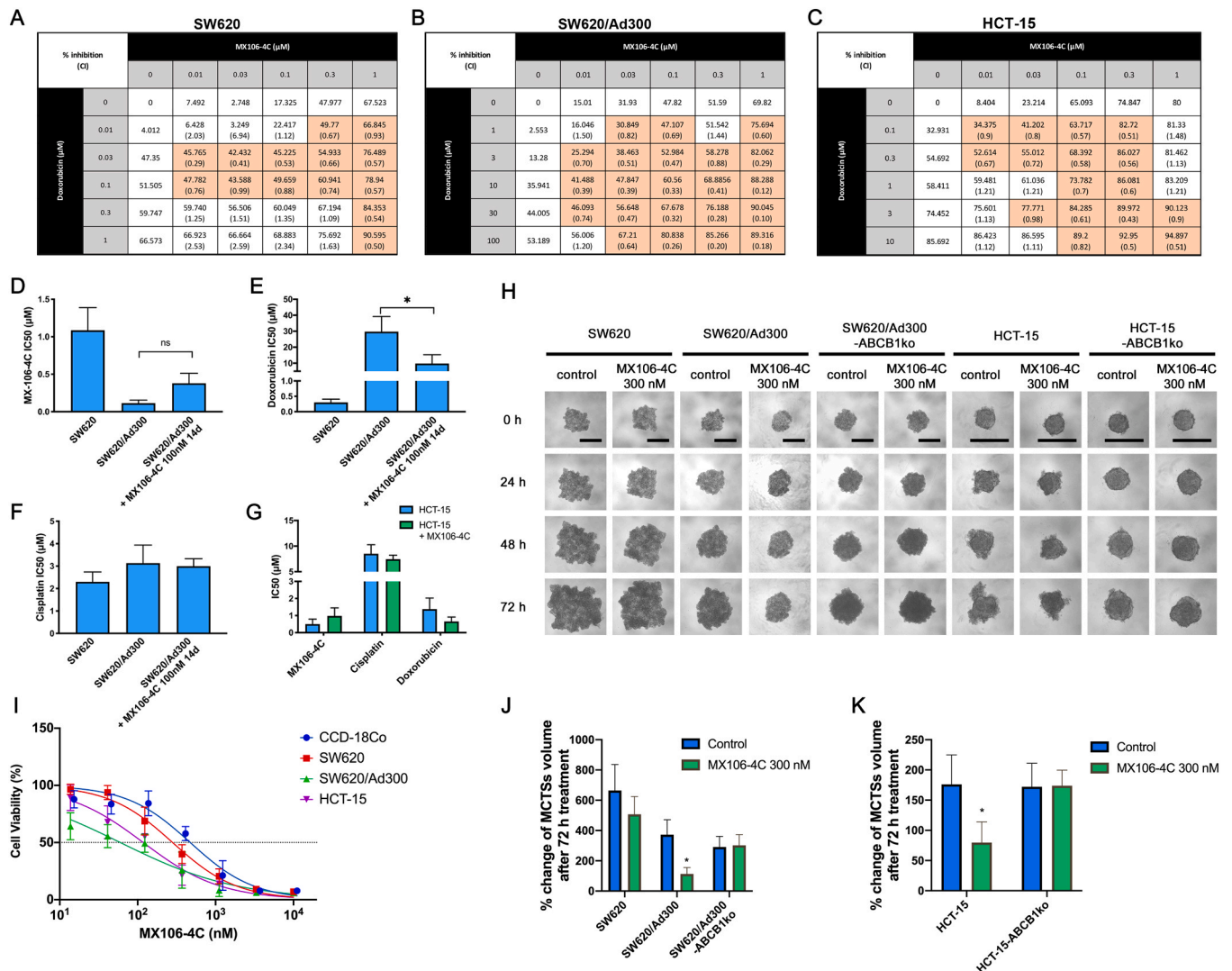


Fig. 7. Anticancer efficacy and safety of MX106-4 C in colorectal cancer cells. (A)-(C) Summary tables for SW620 (A), SW620/Ad300 (B), and HCT-15 (C) cell lines showing potency (% inhibition), combination index (CI), and combination of MX106-4 C and doxorubicin combined at various concentrations and ratios. Combinations exhibiting synergism (CI<1) were highlighted in the table. Data were the average %inhibition obtained from three independent experiments in triplicate. (D)-(G) Effect of 14-day exposure to 100 nM MX106-4 C on drug sensitivity profile of SW620/Ad300 and HCT-15 cells. Columns and error bars represented mean \pm SD of IC₅₀ values determined by MTT assay from three independent experiments in triplicate. * $p < 0.05$. (H) Representative images of the MCTSs treated with either vehicle control (culture media) or 300 nM MX106-4 C at time points 0, 24, 48, and 72 h. The scale bars represented 200 μ m. (I) Comparison on the cytotoxicity of compound MX106-4 C against colorectal cancer cell lines and normal colorectal cell line. Data points with error bars displayed the average viability (%) \pm SD obtained from at least three independent experiments performed in triplicate. (J) (K) Change of MCTSs volumes after treatment. The percentage of MCTSs volume was calculated by (spheroid volume - spheroid volume at timepoint-0)/spheroid volume at timepoint-0 \times 100%. * $p < 0.05$ compared to the control group of the corresponding cell line.

exposure to 100 nM MX106-4 C, SW620/Ad300, and HCT-15 cells gained approximately 3-fold more resistance to the untreated cells (Figs. 7D and 7G). Enhanced sensitivity to ABCB1 substrate doxorubicin was significant in SW620/Ad300 cells after 14-day treatment with MX106-4 C, while HCT-15 cells got less significantly (approximately 2-fold) re-sensitized to doxorubicin by long term exposure to MX106-4 C (Figs. 7E and 7G). This was in accord with the difference in ABCB1 protein level in cells with or without 14-day exposure to MX106-4 C as discussed previously. Cisplatin, which is not transported by ABCB1, was used as a negative control. The IC₅₀ values of cisplatin stayed at a similar level between treated and untreated groups (Figs. 7F and 7G). These results indicated that the low resistance to MX106-4 C and re-sensitization to doxorubicin were associated with the decreased ABCB1 protein expression by long-term treatment of MX106-4 C.

3.11. Selective toxicity of MX106-4 C in ABCB1 overexpressing colorectal cancer multicellular tumor spheroids (MCTSs)

To further evaluate the selective toxicity of MX106-4 C on MDR colorectal cancer cells in a tumor structure, the multicellular tumor spheroid (MCTS) model was used to mimic the natural biology of tumors. It has been reported that MCTSs could have different sensitivity to chemotherapeutic agents compared to 2D monolayer cultured cells because of the differential diffusion of drugs in spheroid structure (Han et al., 2021). Therefore, a preliminary experiment was used to identify the appropriate concentration of MX106-4 C in MCTSs tests. Based on the IC₅₀ values obtained from the MTT assay, three concentrations (100, 300, 1000 nM) were tested in a preliminary experiment, and 300 nM, which was neither too toxic nor too ineffective to all spheroids (data not shown), was selected for further experiment.

As depicted in Fig. 7H, MX106-4 C at 300 nM induced significant

growth inhibition in SW620/Ad300 spheroids, whereas the growth of spheroids from SW620 and SW620/Ad300-ABCB1ko cells was hardly affected. SW620/Ad300 spheroids treated with MX106-4 C had a significantly smaller increase in the diameter of the cell aggregates compared to the control group (Fig. 7J). HCT-15 spheroids treated with MX106-4 C also showed slower growth in diameter compared to the control group, while the growth HCT-15-ABCB1ko spheroids were not affected by 300 nM MX106-4 C (Fig. 7K). Besides of the growth retardation effects, another major observation from HCT-15 spheroid treated with MX106-4 C was the less aggressive growth pattern compared to the control group. The hypersensitivity to MX106-4 C in ABCB1 overexpressing spheroids was consistent with the cytotoxicity effects observed from the MTT assay, suggesting that the selective toxicity of MX106-4 C observed from cell-based assays could be retained in a tumor setting.

3.12. Evaluation on cytotoxicity of MX106-4 C on normal colon cells

To evaluate the safety of compound MX106-4 C, cytotoxicity tests were performed using human normal colon fibroblast cells, CCD-18Co. As shown in Fig. 7I, the inhibitory effect of MX106-4 C on the viability of CCD-18Co cells was less significant compared to the three colorectal cancer cell lines tested. The selectivity index (SI = IC₅₀ from normal cells ÷ IC₅₀ from cancer cells) (Badisa et al., 2009) was calculated to determine the selectivity of MX106-4 C against cancer cells. An SI value higher than 2 suggests selective toxicity against cancer cells and relative safety in normal cells (Awang et al., 2014). As demonstrated in Table 2, the SI values of CCD18Co versus SW620/Ad300 was 19.9 and that of CCD18Co versus HCT-15 was 4.6, indicating that the selectivity of MX106-4 C was good against ABCB1 positive colorectal cancer cells. Since MX106-4 C is a collateral sensitivity agent, the IC₅₀ value of MX106-4 C from SW620 cells with low ABCB1 expression was closer to that from CCD18Co cells, leading to a smaller SI value of 1.6. This suggested that MX106-4 C may be safer to treat ABCB1 positive colorectal cancers.

4. Discussion

The ABCB1 expression is closely correlated with MDR in colorectal cancer, therefore, various approaches to suppress ABCB1 have been developed extensively investigated. As the outcomes for applications of ABCB1 inhibitors in clinical settings have been disappointing, novel strategies are urgently required for surmounting ABCB1-mediated cancer MDR, such as developing novel CS agents that are selectively toxic to ABCB1 overexpressing cancer cells. In this study, the selective toxicity of

Table 2
Cytotoxicity of compound MX106-4 C to normal colorectal cell line and selectivity against colorectal cancer cell lines.

Cell line	MX106-4 C IC ₅₀ ^a (nM)		Selectivity index (SI) ^b
	single drug	+ 1 μM tariquidar	
CCD-18Co	804.19 ± 325.68	948.91 ± 349.93	-
SW620	508.31 ± 57.13	1305.1 ± 434.1	1.6
SW620/Ad300	40.44 ± 3.47	1351.2 ± 506.3	19.9
SW620/Ad300-ABCB1ko	2042.4 ± 315.2	2010.3 ± 672.8	-
HCT-15	175.5 ± 25.2	861.7 ± 144.1	4.6
HCT-15-ABCB1ko	825.2 ± 92.1	916.5 ± 134.9	-

^a IC₅₀: concentration that reduces cell viability by 50% (mean ± SD). Values in the table are determined from at least three independent experiments conducted in triplicate.

^b Selectivity index (SI) = IC₅₀ from normal cells ÷ IC₅₀ from cancer cells. Gene-modified cell lines were not subject to SI calculation.

compound MX106-4 C against ABCB1 positive colorectal cancer cells was characterized and the mechanism of the selective toxicity was investigated.

In the cytotoxicity test, the ABCB1 overexpressing MDR cell lines exhibited resistance to ABCB1 substrate doxorubicin and YM155, while cisplatin, which was used as a non-substrate control of ABCB1, had similar cytotoxic effects on both parental and resistant cell lines. This confirmed the ABCB1-mediated MDR characteristics of the cell models utilized in the present study. MX106-4 C appeared to be a potent CS agent for both intrinsically ABCB1 positive colorectal cancer HCT-15 cells and acquired ABCB1 overexpressing colorectal cancer SW620/Ad300 cells. Sensitivities of cancer cells towards a chemotherapeutic agent are usually correlated with the intracellular concentration. However, the accumulation level of compound MX106-4 C was shown to be comparable in ABCB1 overexpressing SW620/Ad300 cells and the parental SW620 cells, suggesting that the selective toxicity of MX106-4 C was not contributed by increased drug accumulation but by enhanced activities of MX106-4 C specifically in ABCB1-positive colorectal cancer cells. Therefore, MX106-4 C is likely to target a biological molecule that is overexpressed in ABCB1-positive cells or target hyperactive biological events that are dependent on ABCB1 or other molecules overexpressing simultaneously with ABCB1.

From the previous reports, the selective toxicities of CS agents are generally ABCB1-dependent, which could be abrogated by applying an ABCB1 inhibitor or silencing ABCB1 (Laberge et al., 2014; Limniatis and Georges, 2022). Depending on the drug properties, CS agents may interact with ABCB1 directly as a substrate or inhibitor, such as isotetrasin (Abdelfatah et al., 2021), jatrophanes (Reis et al., 2016), and Dp44mT (Jansson et al., 2015) that can stimulate ATP hydrolysis and ROS production, or like verapamil and tamoxifen that can inhibit ABCB1 function thereby disturbing ABCB1-dependent events that are involved cell survival (Limniatis and Georges, 2022). Hence, interaction with ABCB1 was considered as a possible mechanism of action for MX106-4 C. The ABCB1 drug efflux activity can be affected by a substrate or an inhibitor with ATPase stimulating or inhibitory effect, respectively (Nandigama et al., 2019). However, MX106-4 C neither stimulated nor inhibited the ATPase activity of ABCB1, and it did not affect the ABCB1-mediated [³H]-paclitaxel efflux activity, suggesting that it may not be a substrate or typical inhibitor of ABCB1. Nevertheless, the results that the collateral sensitivity effect of MX106-4 C can be reversed by applying ABCB1 inhibitor tariquidar, ABCB1 knockout, or ABCB1 dysfunction mutant indicated a dependence relationship between MX106-4 C-mediated CS effect and functional ABCB1 expression. Therefore, it is likely that MX106-4 C did not interact with ABCB1 directly but interacted with downstream molecules or events that require functional ABCB1.

In particular, it was shown that the TM6,12-14 A mutant with impaired efflux function but normal ATPase function only partially reversed the selective toxicity of MX106-4 C, whereas the TM6,12-14A-EQ mutant with deficient ATPase function completely abolished the selective toxicity, indicating a critical contribution of ATP hydrolysis in the CS effect of MX106-4 C. The involvement of ABCB1-mediated ATP hydrolysis in CS effects has been associated with ROS production (Efferth et al., 2020). The hypothetical mechanism is that when the cells continue to replenish the ATP consumed by ABCB1 ATPase, ADP passes oxidative phosphorylation thereby generating ROS to supplement ATP (Bharathiraja et al., 2023; Karwatsky et al., 2003). As expected according to the finding that the CS effect of MX106-4 C required ABCB1 ATPase activity, it was observed that MX106-4 C could increase ROS generation in SW620/Ad300 cells but not in parental SW620 cells or ABCB1 deficient SW620/Ad300-ABCB1ko cells. Although MX106-4 C was shown to have no direct stimulation on ABCB1 ATPase activity, MX106-4 C could significantly diminish the intracellular ATP levels selectively in ABCB1 overexpressing cells. This discrepancy suggests the existence of an indirect interaction between MX106-4 C and ABCB1, wherein the ATP depletion effect may be contingent upon the

overexpression of ABCB1. The ATPase assay using insect cell membranes may not truly reflect the ABCB1 ATPase activity or specific mechanisms necessary for capturing the ATP depletion effect of MX106-4 C in viable cancer cells. Since exporting activity and ATPase function are suggested as requirements for MX106-4 C-induced CS effect, it can be hypothesized that substrate efflux activity of ABCB1 consuming ATP is ongoing during the process where MX106-4 C exerts toxic effects on cells. The possibility that MX106-4 C causes the generation or release of physiological ABCB1 substrate in cells to indirectly stimulate ABCB1 ATPase cannot be excluded. And the resulting ATP depletion may lead to intensified oxidative phosphorylation required to maintain ATP levels, thereby generating ROS as a side product (Krzyzanowski et al., 2014). Further direct investigation on ATP consumption and ABCB1 ATPase activity is required for confirmation.

The induced ROS production may be a possible explanation for the observation of cell swelling from immunofluorescence microscopic images of SW620/Ad300 cells treated with 100 nM MX106-4 C for 72 h, because ROS accumulation is known to be correlated with mitochondria dysfunction such as calcium overload, mitochondrial permeability transition, and morphological alteration of mitochondria, which can lead to oncotic-like cell death (Ortega-Forte et al., 2022). Nevertheless, whether mitochondria damage is involved in the selective toxicity of MX106-4 C requires further investigation. A time-dependent increase in intracellular ROS levels and a reduction in GSH levels in ABCB1 overexpressing SW620/Ad300 cells treated with MX106-4 C was observed, and these results were also concentration-independent. Albeit increased ROS production in MX106-4 C-treated SW620/Ad300 cells, this turns out to be a minor factor in MX106-4 C-mediated selective toxicity, because coadministration of ROS scavenger NAC replenished intracellular GSH and partially reversed the elevated intracellular ROS levels but failed to counteract the cytotoxicity of MX106-4 C. These findings suggest that the oxidative stress induced by MX106-4 C, while selectively targeting ABCB1 overexpressing cells, may not be the primary mechanism underlying the observed collateral sensitivity effect. The ROS production may be an accompanied phenomenon of ABCB1 activity, which may act as a synergistic contributor rather than a major contributor to the cytotoxicity of MX106-4 C.

Based on the 8-OHQ scaffold in the structure of MX106-4 C, it may bear an iron-chelating character similar to MDR-selective 8-OHQ derivatives such as NSC297366 (Cserepes et al., 2020), which might be a possible contributor to induce oxidative stress and cell death. Contrary to expectations, the treatment with MX106-4 C did not induce iron depletion in the tested cells. Moreover, the presence of iron chelator Bpy or excess iron could not potentiate or attenuate the selective toxicity of MX106-4 C in ABCB1 overexpressing cells (Fig. S6). These findings suggest that, unlike NSC297366, MX106-4 C may not induce iron depletion and may not complex with iron.

Additionally, MX106-4 C may potentially regulate ABCB1 expression. It was found that short-term (up to 72 h) exposure to 100 nM MX106-4 C downregulated ABCB1 expression at mRNA level but not the protein level, while long-term (14 days) exposure significantly reduced ABCB1 protein expression. Similar effects have been reported for the other CS compounds, such as verapamil, KP772 and NSC73306 (Heffeter et al., 2007; Limniatis and Georges, 2022; Ludwig et al., 2006). However, little was known about the mechanism for down-regulating ABCB1 expression in long-term exposure. It could be possible to regulate gene expression pre-transcriptionally. Another possibility is the selection pressure from MX106-4 C. In the field of cancer chemotherapy, it has been suggested that drug resistance can arise through continuous selection for cells that display higher drug tolerance, which exhibit higher stability compared to the sensitive cells and survive upon subsequent cell divisions (Bell and Gilan, 2020; Nik Nabil et al., 2022). Therefore, the loss of ABCB1 expression during long-term exposure could also be caused by the survival advantages of colonies with low ABCB1 expression and further flourishing of such colonies. Further experiments with monitoring ABCB1 expression in cells from the beginning of exposure may help elucidate this question.

Besides interaction with ABCB1, the interaction of MX106-4 C with survivin, which is its designated target, may also contribute to the CS effects. Survivin functions as an inhibitor of apoptosis mainly by binding and inhibiting the activation of caspases-3 and 7 (Garg et al., 2016). In addition, survivin plays a regulatory role in cell cycle progression. It has been reported that overexpression of survivin in human hepatoma cells could interact with CDK4, thereby counteracting G1 arrest and accelerating S phase shift (Suzuki et al., 2000). In order to investigate whether survivin inhibition is involved in the selective toxicity of MX106-4 C, the effects of MX106-4 C on cell cycle arrest, cell apoptosis, and expression of survivin were investigated. The result that MX106-4 C induced cell apoptosis and cell cycle arrest at G0/G1 indicated the survivin inhibition effect exerted by MX106-4 C at 100 nM. The increased level of the active form of caspases-3/7, which are the effector of survivin, was observed in MX106-4 C-treated SW620/Ad300 cells, further confirming survivin inhibition in SW620/Ad300 cells. However, unlike MX106 or other analogs that can degrade survivin (Albadari et al., 2021; Wang et al., 2018a), MX106-4 C did not alter the expression of survivin, which suggested that the inhibitory effect may be functional inhibition instead of regulating the survivin expression. It is also possible that the concentration used is relatively low thus it is not potent enough to degrade survivin. Interestingly, although the survivin expression levels were comparable among SW620, SW620/Ad300, and SW620/Ad300-ABCB1ko cells, the cell cycle arrest at G0/G1 phase and cell apoptosis induced by MX106-4 C at 100 nM selectively occurred in ABCB1 overexpressing SW620/Ad300 cells. Besides, the enhanced activity of cleaved caspases-3/7 in SW620/Ad300 cells could be attenuated by ABCB1 inhibitor tariquidar. This inferred that the survivin functional inhibition by MX106-4 C was also ABCB1-dependent, which may explain why there was mild apoptosis induction in SW620 cells with low ABCB1 expression compared to the unaffected SW620/Ad300-ABCB1ko cells. An unexpected increase in cell populations at the G2/M phase was observed in parental SW620 cells treated with MX106-4 C. As the ABCB1 knockout subline of SW620/Ad300 did not have this type of response, the G2/M phase arrest in SW620 cells induced by MX106-4 C is not likely to be correlated with ABCB1 expression. It may be caused by differential expressions of certain cell cycle-modulating molecules between SW620 and SW620/Ad300 cells that occurred during doxorubicin selection. Nevertheless, the type of cell cycle change appeared to have minimal influence on causing cell death in SW620 cells.

Further bioinformatics analysis revealed that the p53 pathway may be an important player in MX106-4 C induced cell cycle arrest and apoptosis. While the mRNA expression data and subsequent validation indicate a clear impact of MX106-4 C on p53 levels, the exact mechanisms linking MX106-4 C-induced oxidative stress and p53 modulation remain to be elucidated. Survivin, known for its anti-apoptotic role, could potentially be regulated by p53. Unraveling the intricate network of interactions involving MX106-4 C and p53 will provide valuable insights into the molecular mechanisms underpinning the observed selective toxicity, contributing to a more comprehensive understanding of MX106-4 C's mode of action and its potential therapeutic implications. Vital molecules involved in this process may include p21, CDK4, CDK6, and phosphorylated pRb. CDK4/6 are cyclin-dependent kinases responsible for regulating the cycle progression from the G1 phase to the S phase by binding to cyclin D and inactivating phosphorylation of the central tumor suppressor pRb (Bonelli et al., 2019). Phosphorylation on serine-807 and serine-811 of pRb induced by CDK4/6-cyclinD complex leads to functional inactivation of pRb, resulting in cell cycle progression (Topacio et al., 2019), while induction of dephosphorylation leads to apoptosis (Xiong et al., 2019). On the other hand, p21(Cip1/Waf1), which is encoded by the gene CDKN1A, is a CDK inhibitor that regulates cell cycle progression (Engeland, 2022). It has been found that p21 has a complex regulatory function on CDK4/6: it can bind to CDK4/6-cyclinD1 complex, which stabilized and inactivated CDK4/6 function to negatively regulate the G1 to S phase shift; it may in contrast

activate CDK4/6 at low level (Karimian et al., 2016). These cell cycle regulatory molecules may have interactions with survivin. Survivin could interact with CDK4, leading to pRb phosphorylation (Singh et al., 2022). Survivin/CDK4 complex formation may induce p21 released from its complex with CDK4 and interact with mitochondrial procaspase 3 to suppress Fas-mediated cell death (Shan et al., 2021). As supported by the bioinformatic analysis data and further validation results, MX106-4 C may induce cell apoptosis and G0/G1 arrest in SW620/Ad300 cells via down-regulating CDK4 and CDK6 leading to hypophosphorylation of pRb. Although the change in p21 protein level was insignificant, it is still possible that p21 is involved in the MX106-4 C-mediated cell apoptosis mechanism. Inhibition of survivin by MX106-4 C may result in caspase-3-activated cell apoptosis by stabilizing the p21/CDK4 complex and at the same time cause G0/G1 phase arrest. It was clearly observed that functional ABCB1 expression is required for MX106-4 C-mediated cell apoptosis, cell cycle arrest, and the underlying CDK6 inhibition, pRb dephosphorylation and caspase-3 activation. As mutual regulations between survivin and ABCB1 has been found on transcriptional levels but not on translational or post-translational levels in cancer cells (Liu et al., 2010; Shi et al., 2007), survivin and ABCB1 might interact indirectly via involved signaling pathways like the TRAIL apoptotic pathway. However, little has been revealed regarding the precise role of ABCB1 efflux function and ATP hydrolysis in these selective effects from MX106-4 C. Further study is needed to elucidate the roles of ABCB1 and survivin in the CS effect of MX106-4 C.

Finally, as a CS agent, the potential of MX106-4 C to synergistically inhibit heterogenous tumors with conventional anticancer drugs and to re-sensitize heterogenous tumors to ABCB1 substrate drugs was proved. As long-term exposure to MX106-4 C caused significantly reduced expression of ABCB1 in the cell population, it is reasonable that MX106-4 C could re-sensitize colorectal cancer cells to ABCB1 substrate drugs doxorubicin and 5-FU. This ABCB1-specific synergy suggested that MX106-4 C may act as a promising adjuvant to enhance the efficacy of 5-FU in overcoming ABCB1-related resistance in colorectal cancer. Additionally, the finding that oxaliplatin combined with MX106-4 C demonstrated synergistic effects across all tested colorectal cancer cell lines, irrespective of ABCB1 overexpression, indicated mechanisms beyond ABCB1 involvement. As oxaliplatin is a potent inhibitor of survivin (Alotaibi et al., 2017), its combination with MX106-4 C may offer a dual inhibitory effect on survivin, potentially enhancing the therapeutic impact. Oxaliplatin and 5-FU are both first-line chemotherapeutic drugs for colorectal cancer clinical strategy. Therefore, the synergism observed with the combination of MX106-4 C and oxaliplatin or 5-FU strengthens the argument for the potential clinical applicability of MX106-4 C as a combination therapy for drug-resistant colorectal cancer.

Furthermore, considering the limitation of 2D monolayer cell culture that the monolayer culture cells do not reflect the natural structures of tumors and the cell-cell or cell-extracellular environment interactions, and that the drug diffusion patterns are altered (Kapalczyńska et al., 2018), the 3D MCTSs model was used to mimic the tumor growth and sensitivity to MX106-4 C in vitro. It was proved that the selective toxicity of MX106-4 C in vitro can be retained in the 3D spheroid setting. Addressing the potential side effects of MX106-4 C treatment is crucial in evaluating its therapeutic applicability. MX106-4 C, as an experimental compound, could exert unintended effects on normal tissues expressing ABCB1, leading to concerns about toxicity, and as of the present, there is no specific or clear information available regarding its side effects. It is encouraging that MX106-4 C exhibited a good selectivity against ABCB1-positive colorectal cancer cells and was relatively safe for normal colorectal cells. Nevertheless, the normal cell line tested was colorectal fibroblast, whereas ABCB1 is physiologically majorly expressed on the apical epithelial cells of colorectal tissue (Holohan et al., 2013). Therefore, the toxicity of MX106-4 C on colorectal cells expressing ABCB1 remains uncertain. Previously reported data from in

vivo studies using triple-negative breast cancer (TNBC) xenograft models (Wang et al., 2018b) and orthotopic ovarian cancer mouse models (Albadari et al., 2021) have indicated no significant side effects associated with MX106 analogs, underscoring its potential safety profile. Furthermore, these in vivo experiments also have suggested a potential inhibitory effect on metastasis, enhancing the compound's therapeutic appeal. It should be noted that the MCTSs assay in this study primarily aimed at providing a potential clue of the antitumor activity of MX106-4 C, and the relatively simple system in not necessarily representative of the in vivo environment due to the limitations such as possible formation of hypoxic cores that are unlikely to respond to therapies (Evans, 2015). Future study should focus on further evaluation of the anti-cancer efficacy and safety of MX106-4 C in vivo.

5. Conclusion

MX106-4 C is a potent CS agent that selectively kills ABCB1-positive cells without affecting ABCB1 functions or subcellular localization. Mechanistic study findings are illustrated in Fig. 8. The selective toxicity of MX106-4 C is dependent on ABCB1 expression and requires functional ABCB1, particularly ATP hydrolysis, which could explain the ROS production induced by MX106-4 C in ABCB1 overexpressing cells. In addition, the selective cytotoxic effects of MX106-4 C could be associated with ABCB1-dependent functional inhibition on survivin, leading to cell cycle arrest at G0/G1 phase and cell apoptosis, possibly via modulation on p21-CDK4/6-pRb phosphorylation pathway and activation of caspases-3/7. As a CS agent with good selectivity for ABCB1-positive colorectal cancer cells compared to normal colorectal cells, MX106-4 C can be useful to treat colorectal cancer by synergistically killing cancer cells when administrated with doxorubicin or re-sensitizing ABCB1 overexpressing cells to substrate chemotherapeutic drugs.

Ethics statement

Not applicable.

Funding

This research was supported by China Postdoctoral Science

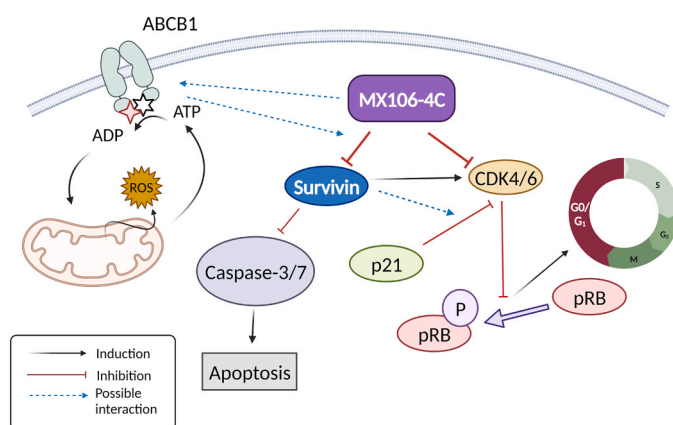


Fig. 8. Graphical summary of possible mechanisms involved in MX106-4 C-induced selective toxicity against ABCB1 positive colorectal cancer cells. The selective toxicity of MX106-4 C depends on ABCB1 expression and requires functional ABCB1, particularly ATP hydrolysis, which could produce ROS in ABCB1 overexpressing cells. The selective cytotoxic effects of MX106-4 C may be associated with ABCB1-dependent functional inhibition on survivin, leading to cell cycle arrest at G0/G1 phase and cell apoptosis, via modulation on p21-CDK4/6-pRb phosphorylation pathway and activation of caspases-3/7. This figure is generated using Biorender.com.

Foundation (No.2023M734064) to Z.L. Additional partial supports were provided by the Department of Pharmaceutical Sciences, St. John's University to Z.S.C, and the University of Tennessee College of Pharmacy Drug Discovery Center to W.L.

CRedit authorship contribution statement

Li Wei: Writing – review & editing, Supervision, Resources, Conceptualization. **Chen Zhe-Sheng:** Writing – review & editing, Supervision, Resources, Conceptualization. **Lei Zi-Ning:** Writing – review & editing, Writing – original draft, Methodology, Investigation, Formal analysis, Data curation, Conceptualization. **Wurpel John N.D.:** Writing – review & editing, Supervision, Resources. **Pan Yihang:** Writing – review & editing, Supervision. **Rahman Hadiar:** Writing – original draft, Methodology, Formal analysis. **Albadari Najah:** Investigation, Formal analysis. **Teng Qiu-Xu:** Writing – original draft, Methodology, Investigation, Formal analysis. **Ma Dejian:** Methodology, Formal analysis. **Ambudkar Suresh V.:** Writing – review & editing, Conceptualization. **Wang Jing-Quan:** Methodology, Formal analysis. **Wu Zhongzhi:** Methodology, Formal analysis.

Declaration of Competing Interest

The authors declare the following financial interests/personal relationships which may be considered as potential competing interests: Dr. Zhe-Sheng Chen is the editor-in-chief, and Dr. Suresh V. Ambudkar is an associate editor of Drug Resistance Updates. If there are other authors, they declare that they have no known competing financial interests or personal relationships that could have appeared to influence the work reported in this paper.

Availability of data and materials

All data are available in the main text or the supplementary materials. The datasets used and/or analyzed during the current study are available from the corresponding author on reasonable request.

Acknowledgments

We thank Dr. Susan E. Bates at Columbia University and Dr. Robert W. Robey at NIH for providing the SW620, SW620/Ad300, and gene transfected HEK293/pcDNA3.1 and HEK293/ABCB1 cell lines. We are thankful to Dr. Diane Hardej from St. John's University for gifting the CCD-18Co cell line.

Appendix A. Supporting information

Supplementary data associated with this article can be found in the online version at [doi:10.1016/j.drug.2024.101065](https://doi.org/10.1016/j.drug.2024.101065).

References

Abdelfatah, S., Bockers, M., Asensio, M., Kadioglu, O., Klinger, A., Fleischer, E., Efferth, T., 2021. Isopetasin and S-isopetasin as novel P-glycoprotein inhibitors against multidrug-resistant cancer cells. *Phytomedicine* 86, 153196.

Albadari, N., Deng, S., Chen, H., Zhao, G., Yue, J., Zhang, S., Miller, D.D., Wu, Z., Li, W., 2021. Synthesis and biological evaluation of selective survivin inhibitors derived from the MX-106 hydroxyquinoline scaffold. *Eur. J. Med. Chem.* 224, 113719.

Albadari, N., Xie, Y., Li, W., 2024. Deciphering treatment resistance in metastatic colorectal cancer: roles of drug transports, EGFR mutations, and HGF/c-MET signaling. *Front. Pharmacol.* 14.

Alotaibi, A.A.A., Najafzadeh, M., Davies, J.D., Baumgartner, A., Anderson, D., 2017. Inhibition of survivin expression after using oxaliplatin and vinflunine to induce cytogenetic damage in vitro in lymphocytes from colon cancer patients and healthy individuals. *Mutagenesis* 32, 517–524.

Amawi, H., Sim, H.-M., Tiwari, A.K., Ambudkar, S.V., Shukla, S., 2019. ABC Transporter-Mediated Multidrug-Resistant Cancer. In: Liu, X., Pan, G. (Eds.), *Drug Transporters in Drug Disposition, Effects and Toxicity*. Springer Singapore, Singapore, pp. 549–580.

Ambudkar, S.V., 1998. Drug-stimulatable ATPase activity in crude membranes of human MDR1-transfected mammalian cells. *ABC Transporters: Biochemical, Cellular, and Molecular Aspects*. Academic Press, pp. 504–514.

Awang, N., Aziz, Z.A., Kamaludin, N.F., Chan, K.M., 2014. Cytotoxicity and mode of cell death induced by Triphenyltin (IV) compounds in vitro. *Online. J. Biol. Sci.* 14, 84–93.

Badisa, R.B., Darling-Reed, S.F., Joseph, P., Cooperwood, J.S., Latinwo, L.M., Goodman, C.B., 2009. Selective cytotoxic activities of two novel synthetic drugs on human breast carcinoma MCF-7 cells. *Anticancer Res.* 29, 2993–2996.

Bell, C.C., Gilan, O., 2020. Principles and mechanisms of non-genetic resistance in cancer. *Br. J. Cancer* 122, 465–472.

Bharathiraja, P., Yadav, P., Sajid, A., Ambudkar, S.V., Prasad, N.R., 2023. Natural medicinal compounds target signal transduction pathways to overcome ABC drug efflux transporter-mediated multidrug resistance in cancer. *Drug Resist. Updates* 71, 101004.

Bonelli, M., La Monica, S., Fumarola, C., Alfieri, R., 2019. Multiple effects of CDK4/6 inhibition in cancer: From cell cycle arrest to immunomodulation. *Biochem. Pharmacol.* 170, 113676.

Chou, T.-C., 2010. Drug combination studies and their synergy quantification using the Chou-Talalay method. *Cancer Res.* 70, 440–446.

Cserepes, M., Turk, D., Toth, S., Pape, V.F.S., Gaal, A., Gera, M., Szabo, J.E., Kucsma, N., Varady, G., Vertessy, B.G., Strelci, C., Szabo, P.T., Tovari, J., Szoboszlai, N., Szakacs, G., 2020. Unshielding multidrug resistant cancer through selective iron depletion of P-glycoprotein-expressing cells. *Cancer Res.* 80, 663–674.

Efferth, T., Saeed, M.E.M., Kadioglu, O., Seo, E.-J., Shirooie, S., Mbaveng, A.T., Nabavi, S.M., Kuete, V., 2020. Collateral sensitivity of natural products in drug-resistant cancer cells. *Biotechnol. Adv.* 38, 107342.

Engeland, K., 2022. Cell cycle regulation: p53-p21-RB signaling. *Cell Death Differ.* 29, 946–960.

Evans, C.L., 2015. Three-dimensional in vitro cancer spheroid models for photodynamic therapy: strengths and opportunities. *Front. Phys.* 3, 15.

Furedi, A., Toth, S., Szebenyi, K., Pape, V.F.S., Turk, D., Kucsma, N., Cervenak, L., Tovari, J., Szakacs, G., 2017. Identification and validation of compounds selectively killing resistant cancer: delineating cell line-specific effects from P-glycoprotein-induced toxicity. *Mol. Cancer Ther.* 16, 45–56.

Garg, H., Suri, P., Gupta, J.C., Talwar, G.P., Dubey, S., 2016. Survivin: a unique target for tumor therapy. *Cancer Cell Int.* 16, 49.

Han, S.J., Kwon, S., Kim, K.S., 2021. Challenges of applying multicellular tumor spheroids in preclinical phase. *Cancer Cell Int.* 21, 152.

Hefeter, P., Jakupec, M.A., Korner, W., Chiba, P., Pirker, C., Dornetshuber, R., Elbling, L., Sutterluty, H., Micksche, M., Keppler, B.K., Berger, W., 2007. Multidrug-resistant cancer cells are preferential targets of the new antineoplastic lanthanum compound KP772 (FFC24). *Biochem. Pharmacol.* 73, 1873–1886.

Holohan, C., Van Schaeybroeck, S., Longley, D.B., Johnston, P.G., 2013. Cancer drug resistance: an evolving paradigm. *Nat. Rev. Cancer* 13, 714–726.

Jansson, P.-J., Yamagishi, T., Arvind, A., Seebacher, N., Gutierrez, E., Stacy, A., Maleki, S., Sharp, D., Sahni, S., Richardson, D.R., 2015. Di-2-pyridylketone 4,4-dimethyl-3-thiosemicarbazone (Dp44mT) overcomes multidrug resistance by a novel mechanism involving the hijacking of lysosomal P-glycoprotein (pgp). *J. Biol. Chem.* 290, 9588–9603.

Ji, N., Yang, Y., Cai, C.-Y., Lei, Z.-N., Wang, J.-Q., Gupta, P., Shukla, S., Ambudkar, S.V., Kong, D., Chen, Z.-S., 2019. Selonsertib (GS-4997), an ASK1 inhibitor, antagonizes multidrug resistance in ABCB1- and ABCG2-overexpressing cancer cells. *Cancer Lett.* 440-441, 82–93.

Kapalczyńska, M., Kolenda, T., Przybyła, W., Zajackowska, M., Teresiak, A., Filas, V., Ibbs, M., Blizniak, R., Luczewski, L., Lamperska, K., 2018. 2D and 3D cell cultures - a comparison of different types of cancer cell cultures. *Arch. Med. Sci.* 14, 910–919.

Karimian, A., Ahmadi, Y., Yousefi, B., 2016. Multiple functions of p21 in cell cycle, apoptosis and transcriptional regulation after DNA damage. *DNA Repair (Amst.)* 42, 63–71.

Karthika, C., Sureshkumar, R., Zehravi, M., Akter, R., Ali, F., Ramproshad, S., Mondal, B., Kundu, M.K., Dey, A., Rahman, M.H., Antonescu, A., Cavalu, S., 2022. Multidrug resistance in cancer cells: focus on a possible strategy plan to address colon carcinoma cells. *Life (Basel)* 12, 811.

Karwatsky, J., Lincoln, M.C., Georges, E., 2003. A mechanism for P-glycoprotein-mediated apoptosis as revealed by verapamil hypersensitivity. *Biochemistry* 42, 12163–12173.

Krzyzanowski, D., Bartosz, G., Grzelak, A., 2014. Collateral sensitivity: ABCG2-overexpressing cells are more vulnerable to oxidative stress. *Free Radic. Biol. Med.* 76, 47–52.

Laberge, R.-M., Ambadipudi, R., Georges, E., 2014. P-glycoprotein mediates the collateral sensitivity of multidrug resistant cells to steroid hormones. *Biochem. Biophys. Res. Commun.* 447, 574–579.

Lei, Z.-N., Teng, Q.-X., Wu, Z.-X., Ping, F.-F., Song, P., Wurpel, J.N.D., Chen, Z.-S., 2021. Overcoming multidrug resistance by knock-out of ABCB1 gene using CRISPR/Cas9 system in SW620/Ad300 colorectal cancer cells. *MedComm (2020)* 2, 765–777.

Liao, D., Zhang, W., Gupta, P., Lei, Z.-N., Wang, J.-Q., Cai, C.-Y., Vera, A.A.D., Zhang, L., Chen, Z.-S., Yang, D.-H., 2019. Tetrandrine Interaction with ABCB1 reverses multidrug resistance in cancer cells through competition with anti-cancer drugs followed by downregulation of ABCB1 expression. *Molecules* 24, 4383.

Limniatis, G., Georges, E., 2022. Down-regulation of ABCB1 by collateral sensitivity drugs reverses multidrug resistance and up-regulates enolase I. *J. Biochem.* 172, 37–48.

Liu, F., Liu, S., He, S., Xie, Z., Zu, X., Jiang, Y., 2010. Survivin transcription is associated with P-glycoprotein/MDR1 overexpression in the multidrug resistance of MCF-7 breast cancer cells. *Oncol. Rep.* 23, 1469–1475.

- Ludwig, J.A., Szakacs, G., Martin, S.E., Chu, B.F., Cardarelli, C., Sauna, Z.E., Caplen, N.J., Fales, H.M., Ambudkar, S.V., Weinstein, J.N., Gottesman, M.M., 2006. Selective toxicity of NSC73306 in MDR1-positive cells as a new strategy to circumvent multidrug resistance in cancer. *Cancer Res.* 66, 4808–4815.
- Morgan, E., Arnold, M., Gini, A., Lorenzoni, V., Cabasag, C.J., Laversanne, M., Vignat, J., Ferlay, J., Murphy, N., Bray, F., 2023. Global burden of colorectal cancer in 2020 and 2040: incidence and mortality estimates from GLOBOCAN. *Gut* 72, 338–344.
- Musyuni, P., Bai, J., Sheikh, A., Vasanthan, K.S., Jain, G.K., Abourehab, M.A.S., Lather, V., Aggarwal, G., Kesharwani, P., Pandita, D., 2022. Precision medicine: Ray of hope in overcoming cancer multidrug resistance. *Drug Resist. Updates* 65, 100889.
- Nandigama, K., Lusvarghi, S., Shukla, S., Ambudkar, S.V., 2019. Large-scale purification of functional human P-glycoprotein (ABCB1). *Protein Expr. Purif.* 159, 60–68.
- Narayanan, S., Gupta, P., Nazim, U., Ali, M., Karadkhelkar, N., Ahmad, M., Chen, Z.-S., 2019. Anti-cancer effect of Indanone-based thiazolyl hydrazone derivative on colon cancer cell lines. *Int J. Biochem Cell Biol.* 110, 21–28.
- Nik Nabil, W.N., Xi, Z., Liu, M., Li, Y., Yao, M., Liu, T., Dong, Q., Xu, H., 2022. Advances in therapeutic agents targeting quiescent cancer cells, *Acta Mater. Medica* 1, 56–71.
- Ortega-Forte, E., Hernandez-Garcia, S., Viguera, G., Henarejos-Escudero, P., Cutillas, N., Ruiz, J., Gandia-Herrero, F., 2022. Potent anticancer activity of a novel iridium metalloid drug via oncosis. *Cell Mol. Life Sci.* 79, 510.
- Pape, V.F.S., Palko, R., Toth, S., Szabo, M.J., Sessler, J., Dorman, G., Enyedy, E.A., Soos, T., Szatmari, I., Szakacs, G., 2022. Structure-activity relationships of 8-hydroxyquinoline-derived mannich bases with tertiary amines targeting multidrug-resistant cancer. *J. Med. Chem.* 65, 7729–7745.
- Pluchino, K.M., Hall, M.D., Goldsborough, A.S., Callaghan, R., Gottesman, M.M., 2012. Collateral sensitivity as a strategy against cancer multidrug resistance. *Drug Resist Updat* 15, 98–105.
- Reis, M.A., Ahmed, O.B., Spengler, G., Molnar, J., Lage, H., Ferreira, M.-J.U., 2016. Jatropane diterpenes and cancer multidrug resistance - ABCB1 efflux modulation and selective cell death induction. *Phytomedicine* 23, 968–978.
- Sajid, A., Lusvarghi, S., Murakami, M., Chufan, E.E., Abel, B., Gottesman, M.M., Durell, S.R., Ambudkar, S.V., 2020. Reversing the direction of drug transport mediated by the human multidrug transporter P-glycoprotein. *Proc. Natl. Acad. Sci. USA* 117, 29609–29617.
- Shan, Y., Li, Y., Han, H., Jiang, C., Zhang, H., Hu, J., Sun, H., Zhu, J., 2021. Insulin reverses choriocarcinoma 5-fluorouracil resistance. *Bioengineered* 12, 2087–2094.
- Shi, Z., Liang, Y.-J., Chen, Z.-S., Wang, X.-H., Ding, Y., Chen, L.-M., Fu, L.-W., 2007. Overexpression of Survivin and XIAP in MDR cancer cells unrelated to P-glycoprotein. *Oncol. Rep.* 17, 969–976.
- Singh, A., Spitzer, M.H., Joy, J.P., Kaileh, M., Qiu, X., Nolan, G.P., Sen, R., 2022. Postmitotic G1 phase survivin drives mitogen-independent cell division of B lymphocytes. *Proc. Natl. Acad. Sci. USA* 119, e2115567119.
- Suzuki, A., Hayashida, M., Ito, T., Kawano, H., Nakano, T., Miura, M., Akahane, K., Shiraki, K., 2000. Survivin initiates cell cycle entry by the competitive interaction with Cdk4/p16(INK4a) and Cdk2/cyclin E complex activation. *Oncogene* 19, 3225–3234.
- Szakacs, G., Annerau, J.-P., Lababidi, S., Shankavaram, U., Arciello, A., Bussey, K.J., Reinhold, W., Guo, Y., Kruh, G.D., Reimers, M., Weinstein, J.N., Gottesman, M.M., 2004. Predicting drug sensitivity and resistance: profiling ABC transporter genes in cancer cells. *Cancer Cell* 6, 129–137.
- Szakacs, G., Hall, M.D., Gottesman, M.M., Boumendjel, A., Kachadourian, R., Day, B.J., Baubichon-Cortay, H., Di Pietro, A., 2014. Targeting the Achilles heel of multidrug-resistant cancer by exploiting the fitness cost of resistance. *Chem. Rev.* 114, 5753–5774.
- To, K.K.W., Wu, M., Tong, C.W.S., Yan, W., 2020. Drug transporters in the development of multidrug resistance in colorectal cancer. In: Cho, C.H., Hu, T. (Eds.), *Drug Resistance in Colorectal Cancer: Molecular Mechanisms and Therapeutic Strategies*. Academic Press, pp. 35–55.
- Topacio, B.R., Zatulovskiy, E., Cristea, S., Xie, S., Tambo, C.S., Rubin, S.M., Sage, J., Koivomagi, M., Skotheim, J.M., 2019. Cyclin D-Cdk4,6 drives cell-cycle progression via the retinoblastoma protein's C-terminal helix. *Mol. Cell* 74, 758–770 e754.
- Wang, C.C., Wang, J.-Y., Lee, T.-E., Cheng, Y.-Y., Morris-Natschke, S.L., Lee, K.-H., Hung, C.-C., 2019. Tenulin and isotenulin inhibit P-glycoprotein function and overcome multidrug resistance in cancer cells. *Phytomedicine* 53, 252–262.
- Wang, Q., Arnt, K.E., Xue, Y., Lei, Z.-N., Ma, D., Chen, Z.-S., Miller, D.D., Li, W., 2018a. Synthesis and biological evaluation of indole-based UC-112 analogs as potent and selective survivin inhibitors. *Eur. J. Med. Chem.* 149, 211–224.
- Wang, Q., Shen, X., Chen, G., Du, J., 2022. Drug resistance in colorectal cancer: from mechanism to clinic. *Cancers (Basel)* 14, 2928.
- Wang, W., Zhang, B., Mani, A.M., Wu, Z., Fan, Y., Li, W., Wu, Z.-H., 2018b. Survivin inhibitors mitigate chemotherapeutic resistance in breast cancer cells by suppressing genotoxic nuclear factor-kappaB activation. *J. Pharm. Exp. Ther.* 366, 184–193.
- Xiao, M., Xue, Y., Wu, Z., Lei, Z.-N., Wang, J., Chen, Z.-S., Li, W., 2019. Design, synthesis and biological evaluation of selective survivin inhibitors. *J. Biomed. Res* 33, 82–100.
- M. Xiao, Y. Xue, Z. Wu, Z.-N. Lei, J. Wang, Z.-S. Chen and W. Li, *Design, synthesis and biological evaluation of selective survivin inhibitors*, (2017).
- Xiong, Y., Li, T., Assani, G., Ling, H., Zhou, Q., Zeng, Y., Zhou, F., Zhou, Y., 2019. Ribociclib, a selective cyclin D kinase 4/6 inhibitor, inhibits proliferation and induces apoptosis of human cervical cancer in vitro and in vivo. *Biomed. Pharm.* 112, 108602.
- Yang, Y., Ji, N., Cai, C.-Y., Wang, J.-Q., Lei, Z.-N., Teng, Q.-X., Wu, Z.-X., Cui, Q., Pan, Y., Chen, Z.-S., 2020. Modulating the function of ABCB1: in vitro and in vivo characterization of sitravatinib, a tyrosine kinase inhibitor. *Cancer Commun. (Lond.)* 40, 285–300.
- Zhang, H., Xu, H., Ashby Jr., C.R., Assaraf, Y.G., Chen, Z.-S., Liu, H.-M., 2021. Chemical molecular-based approach to overcome multidrug resistance in cancer by targeting P-glycoprotein (P-gp). *Med. Res. Rev.* 41, 525–555.